ƒ ‹ F | Œfia‹ ˙'e›ß• |–M^D‹ ª¤s›p e ƒ¤"G‡ł§i

›†˜ı⁄ ¶§'° † ›M ƒ¤⁄ Peptidoglycan¤°¿E¥¤ ‰† ›M«e o

"¢"«‰Ł˜ 'æ⁄§ Tfi§¶˙»…–• Q(3/3)

›p e^ §¡G §O«‹›p e

›p e‰ ¸s„¡GNSC94-2320-B-038-033-

ıƒ • ¶¡¡G94 ƒ~08⁄°01⁄ ƒ 95 ƒ~07⁄°31⁄Ø

ıƒ ‡ ƒ ¡G» O ¥´ ˙⁄j ˙´ ¤ § ‡N¤t

›p e¥ D ø⁄¡HG" L «•

ƒ ƒP¥ D ø⁄¡HG‡ fl ←–`

›p e »P⁄H›ß¡G, ¶ fi ¢ ¡ B – d ƒ¶v¡B„ø†fi§g

‡ł§i^ «‹¡G§ „ª‡ł§i

‡ B † zŁ¡fG¡¥»›p e¥ i ⁄ ‰ ¶‹ d,

⁄⁄ ¥` Œ 95 ƒ~9⁄°18⁄Ø

行政院國家科學委員會補助專題研究計畫■成果報告
期中進度報告

革蘭氏陽性菌細胞壁成分 Peptidoglycan 刺激巨噬細胞前發炎物質釋放之訊息傳遞探討(3/3)

計畫類別：■ 個別型計畫　　整合型計畫
計畫編號：NSC　94－2320－B－038－033-
執行期間：　94 年　8 月　1 日至 94 年　7 月 31 日

計畫主持人：林建煌
共同主持人：陳炳常
計畫參與人員：詹雅璇、康如鈞、廖皎君

成果報告類型(依經費核定清單規定繳交)：□精簡報告 ■完整報告

本成果報告包括以下應繳交之附件：
□赴國外出差或研習心得報告一份
□赴大陸地區出差或研習心得報告一份
□出席國際學術會議心得報告及發表之論文各一份
□國際合作研究計畫國外研究報告書一份

處理方式：除產學合作研究計畫、提升產業技術及人才培育研究計畫、列管計畫及下列情形者外，得立即公開查詢
□涉及專利或其他智慧財產權，□一年□二年後可公開查詢

執行單位：台北醫學大學醫事技術學系

中　華　民　國　95　年　9　月　7　日

英文摘要。

關 鍵 字 ： Inflammation, Transcription Factors, Cytokines, Lipid Mediators, Monocytes/Macrophages。

In this study, we investigated the signaling pathway involved in interleukin-6 (IL-6) production caused by peptidoglycan (PGN), a cell wall component of the gram-positive bacterium, *Staphylococcus aureus*, in RAW 264.7 macrophages. PGN caused concentration- and time-dependent increases in IL-6, PGE_2 and cAMP production. PGN-mediated IL-6 production was inhibited by a non-selective cyclooxygenase (COX) inhibitor (indomethacin), a selective COX-2 inhibitor (NS398), an EP2 antagonist (AH6809), an EP4 antagonist (AH23848), and a protein kinase A (PKA) inhibitor (KT5720), but not by a non-selective nitric oxide synthase inhibitor (N^G-nitro-arginine methyl ester). Furthermore, PGE_2, an EP2 agonist (butaprost), an EP2/EP3/EP4 agonist (misoprostol), and misoprostol in the presence of AH6809 all induced IL-6 production, whereas an EP1/EP3 agonist (sulprostone) did not. PGN caused time-dependent activations of IκB kinase α/β and p65 phosphorylation at Ser276, and these effects were inhibited by NS398 and KT5720. Both PGE_2 and 8-bromo-cAMP, also caused IKKα/β phosphorylation. PGN resulted in two “waves” of the formation of NF-κB-specific DNA-protein complexes. The first wave of NF-κB activation occurred at 10~60 min of treatment, while the later wave occurred at 2~12 h of treatment. The PGN-induced increase in κB-luciferase activity was inhibited by NS398, AH6809, AH23848, KT5720, a PKC inhibitor (Ro31-8220), and a p38 MAPK inhibitor (SB203580). These results suggest that PGN-induced IL-6 production involves COX-2-generated PGE_2, activation of the EP2 and EP4 receptors, cAMP formation, and the activation of PKA, PKC, p38 MAPK, IKKα/β, p65 phosphorylation, and NF-κB. However, PGN-induced nitric oxide release is not involved in the signaling pathway of PGN-induced IL-6 production.

中文摘要。

關鍵字：Inflammation, Transcription Factors, Cytokines, Lipid Mediators, Monocytes/Macrophages。發炎;轉錄因子;細胞激素巨;脂質媒介物質;單核球/噬細胞。

在本研究中，我們將探討革蘭氏陽性菌細胞壁成分peptidoglycan (PGN)誘導RAW 264.7巨噬細胞IL-6產生之訊息傳遞路徑。PGN依劑量及時間相關曲線增加IL-6、PGE_2及cAMP的產生。PGN媒介IL-6產生可被非選擇性COX抑制劑(indomethacin)、選擇性COX抑制劑(NS398)、PGE_2 (EP2)拮抗劑(AH6809)、EP4拮抗劑(AH23848)及protein kinase A抑制劑(KT5720)所抑劑，但不受非選擇性NO synthase抑制劑(N^G-nitro-arginine methyl ester)所抑制。更進一步PGE_2、EP2作用劑(butaprost)、EP2/PGE_3 (EP3)/EP4作用劑(mioprostol)及具有AH6809與mioprostol共同存在下皆可誘導IL-6產生，然而EP1/EP3作用劑(sulprostone)則不會。PGN可以依照時間曲線活化IκB kinase α/β (IKKα/β)及p65之Ser276之磷酸化，這些作用可被NS398及KT5720所抑制。PGE_2及8-bromo-cAMP二者也可以誘導IKKα/β之磷酸化。PGN可以依二項增加NF-κB-特異DNA-蛋白複合物的形成，第一項NF-κB的活化發生在10-60分，而第二項則發生在2-12小時。PGN增加κB-luciferase的活性可被NS398、AH6809、AH23848、KT5720、protein kinase C抑制劑(Ro31-8220)及p38 MAPK抑制劑(SB203580)所抑制。經由以上的結果發現PGN誘導IL-6的產生其中包含COX-2產生PGE_2、活化EP2/EP4受體、cAMP形成、活化PKA、PKC、p38 MAPK、IKKα/β、p65磷酸化及NF-κB。然而PGN誘導NO釋放並不參與在PGN誘導IL-6的產生。

報告內容[前言及文獻探討、研究目的、研究方法、結果與討論(含結論與建議)]

本研究計劃第一年的成果目前已經發表在The Journal of Biological Chemistry (2004) Vol. 279, No. 20, Issue of May 14, pp20889-20897的期刊中，請見所附之期刊內容。第二年的成果目前已經在Molecular Immunology期刊 revised中。第三年的成果目前已經發表在The Journal of Immunology (2006) 177:681-693的期刊中，請見所附之期刊內容。經由本計劃之執行與研究，必定能清楚明瞭在革蘭氏陽性菌感染時所產生的發炎現象。因此，藉由本計劃的完成將能尋找出治療革蘭氏陽性菌的治療方針。

Peptidoglycan-Induced IL-6 Production in RAW 264.7 Macrophages Is Mediated by Cyclooxygenase-2, PGE_2/PGE_4 Receptors, Protein Kinase A, IκB Kinase, and NF-κB[1]

Bing-Chang Chen,* Chiao-Chun Liao,† Ming-Jen Hsu,‡ Yi-Ting Liao,‡ Chia-Chin Lin,§ Joen-Rong Sheu,‡ and Chien-Huang Lin[2‡]

In this study, we investigated the signaling pathway involved in IL-6 production caused by peptidoglycan (PGN), a cell wall component of the Gram-positive bacterium, *Staphylococcus aureus*, in RAW 264.7 macrophages. PGN caused concentration- and time-dependent increases in IL-6, PGE_2, and cAMP production. PGN-mediated IL-6 production was inhibited by a nonselective cyclooxygenase (COX) inhibitor (indomethacin), a selective COX-2 inhibitor (NS398), a PGE_2 (EP2) antagonist (AH6809), a PGE_4 (EP4) antagonist (AH23848), and a protein kinase A (PKA) inhibitor (KT5720), but not by a nonselective NO synthase inhibitor (N^G-nitro-L-arginine methyl ester). Furthermore, PGE_2, an EP2 agonist (butaprost), an EP2/PGE_3 (EP3)/EP4 agonist (misoprostol), and misoprostol in the presence of AH6809 all induced IL-6 production, whereas an EP1/EP3 agonist (sulprostone) did not. PGN caused time-dependent activations of IκB kinase αβ (IKKdβ) and p65 phosphorylation at Ser^{276}, and these effects were inhibited by NS398 and KT5720. Both PGE_2 and 8-bromo-cAMP also caused IKKdβ kinase αβ phosphorylation. PGN resulted in two waves of the formation of NF-κB-specific DNA-protein complexes. The first wave of NF-κB activation occurred at 10–60 min of treatment, whereas the later wave occurred at 2–12 h of treatment. The PGN-induced increase in κB luciferase activity was inhibited by NS398, AH6809, AH23848, KT5720, a protein kinase C inhibitor (Ro31-8220), and a p38 MAPK inhibitor (SB203580). These results suggest that PGN-induced IL-6 production involves COX-2-generated PGE_2, activation of the EP2 and EP4 receptors, cAMP formation, and the activation of PKA, protein kinase C, p38 MAPK, IKKdβ, kinase αβ, p65 phosphorylation, and NF-κB. However, PGN-induced NO release is not involved in the signaling pathway of PGN-induced IL-6 production. ***The Journal of Immunology,*** **2006, 177: 681–693.**

Bacteria stimulate the innate immune system of a host and the release of inflammatory molecules such as cytokines and chemokines as a response to infections (1, 2). LPS is a well-known activator of the innate immune system in Gram-negative infections (3). During Gram-positive infections, when no endotoxin is present, peptidoglycan (PGN),[3] the major component of the cell wall of Gram-positive bacteria, activates the innate immune system of the host and induces the release of cytokines (TNF-α, IL-1, and IL-6) and chemokines (IL-8/CXCL8, MIP-1, MIP-2, and MCP) (3–5). These inflammatory molecules are the major cause of the various signs and symptoms that occur during bacterial infections, including fever, inflammation, and acute phase responses (3–5).

IL-6 is a multifunctional cytokine that plays a central role in both innate and acquired immune responses. IL-6 is the predominant mediator of the acute phase response, an innate immune mechanism which is triggered by infection and inflammation (6, 7). IL-6 also plays multiple roles during the subsequent development of acquired immunity against incoming pathogens, including regulation of the expressions of cytokine and chemokine, stimulation of Ab production by B cells, regulation of macrophage and dendritic cell differentiation, and the response of regulatory T cells to microbial infection (6, 7). In addition to these roles in pathogen-specific inflammation and immunity, IL-6 levels are elevated in chronic inflammatory conditions, such as rheumatoid arthritis (8–10). Several consensus sequences, including those for NF-κB, CREB, NF-IL-6, and AP-1 in the 5′ promoter region of the *IL-6* gene, have been identified as regulatory sequences that induce IL-6 in response to various stimuli (11, 12). NF-κB, a key transcription factor that regulates IL-6 expression, is a dimer of either transcription factor p65 or transcription factor p50 (13). In a resting state, this dimer is associated with IκBs to retain NF-κB in the cytosol (14). IκB kinase (IKK), which is activated through stimulation by cytokines and bacterial products, phosphorylates IκBα at Ser^{32} and Ser^{36} and IκBβ at Ser^{19} and Ser^{23} (15–17), to produce ubiquitination of IκBαβ at lysine residues and degradation by the 26S proteasome (18). This process releases active NF-κB, which is then translocated from the cytosol to the nucleus, to bind specific DNA enhancer sequences and induce gene transcription (13). Regulation of IκB degradation and the subsequent release of NF-κB constitute a critical control point in the pathway. However, recent results suggest that an additional IκB-independent pathway is activated, which causes the enhanced transactivation potential of NF-κB once it is bound to its consensus sequence (19, 20). Activation of the pathway has been shown to result in increased

*School of Respiratory Therapy, Graduate Institutes of †Biomedical Technology and ‡Medical Sciences, College of Medicine, Taipei Medical University, Taipei, Taiwan; and §Graduate Institute of Nursing, College of Nursing, Taipei Medical University, Taipei, Taiwan

Received for publication May 19, 2005. Accepted for publication April 14, 2006.

The costs of publication of this article were defrayed in part by the payment of page charges. This article must therefore be hereby marked *advertisement* in accordance with 18 U.S.C. Section 1734 solely to indicate this fact.

[1] This work was supported by Grant NSC 93-2314-B-038-014 from the National Science Council of Taiwan.

[2] Address correspondence and reprint requests to Dr. Chien-Huang Lin, Graduate Institute of Medical Sciences, College of Medicine, Taipei Medical University, 250 Wu-Hsing Street, Taipei 110, Taiwan. E-mail address: chlin@tmu.edu.tw

[3] Abbreviations used in this paper: PGN, peptidoglycan; COX-2, cyclooxygenase 2; EP, PGE_2 receptor; IKKαβ, IκB kinase αβ; iNOS, inducible nitric oxide synthase; L-NAME, N^G-nitro-L-arginine methyl ester; PDTC, pyrrolidine dithiocarbamate; PKA, protein kinase A; PKC, protein kinase C; TP, thromboxane A_2 receptor.

Copyright © 2006 by The American Association of Immunologists, Inc.

0022-1767/06/$02.00

phosphorylation of the p65 (RelA) subunit of NF-κB and to promote interaction of p65 with the coactivator protein, p300/CBP (21–23).

PGs are ubiquitous compounds involved in a variety of homeostatic and inflammatory processes (24). They are formed by the combined action of phospholipase A_2, which liberates arachidonic acid from the *sn*-2 position of cellular membrane phospholipids, and cyclooxygenase (COX), which converts arachidonic acid to the endoperoxide intermediate, PGH_2. PGH_2 is then subsequently converted to various PGs by the action of cell-specific synthases (24). COX-2 is a COX isoform that is induced in a number of cells by proinflammatory stimuli and is thought to contribute to the generation of prostanoids at sites of inflammation (25, 26). It is considered to be responsible for the high production of PGs (27). PGE_2, one of the major PGs produced, exerts its biological effects by binding to specific cell surface receptors, designated PGE_2 receptors (EPs). There are four different EPs that have been identified, named EP1 to EP4, and several splice variants of EP3 are known (28). Activation of EPs leads to well-defined alterations in intracellular calcium and cAMP concentrations; e.g., Gs-coupled cAMP increases via adenylyl cyclase activation by EP2 and EP4, and intracellular calcium increases via phosphatidylinositol turnover by EP1, whereas a Gi-coupled decrease in cAMP is effected by EP3 (29). Therefore, many different physiological processes are regulated by PGE_2 activation of specific receptor subtypes.

Previous studies have shown a positive association between endogenous PGE_2 production and IL-6 synthesis both in vitro (30–33) and in vivo (31, 34). However, the signaling pathway between COX-2 induction and IL-6 release by PGN stimulation is still unknown. A recent study from our laboratory showed that PGN induces TLR2, p85α, and Ras complex formation and subsequently activates the Ras/Raf-1/ERK pathway, which in turn initiates IKKαβ and NF-κB activation, and ultimately induces COX-2 expression in RAW 264.7 macrophages (35). In the present study, RAW 264.7 macrophages were exposed to PGN, and the signaling pathway between COX-2 induction and IL-6 production was investigated. Our studies demonstrated that in RAW 264.7 macrophages, PGN stimulates IL-6 production by a COX-2/PGE_2-dependent mechanism. We show that EP2/EP4, intracellular cAMP formation, and the activation of PKA, protein kinase C (PKC), p38 MAPK, IKKαβ, p65 phosphorylation, and NF-κB are involved in PGN-stimulated IL-6 production. However, PGN-induced NO release is not involved in the signaling pathway of PGN-induced IL-6 production.

Materials and Methods

Materials

PGN (derived from *Staphylococcus aureus*) was purchased from Fluka. LPS (derived from *Escherichia coli*), N^G-nitro-L-arginine methyl ester (L-NAME), polymyxin B, AH23848, and misoprostol were purchased from Sigma-Aldrich. NS398, KT5720, Ro31-8220, SB203580, and 8-bromo-cAMP were obtained from Calbiochem. PGE_2, AH6809, butaprost, sulprostone, and the IL-6, PGE_2, and cAMP enzyme immunoassay kits were obtained from Cayman. DMEM/Ham's F-12, FCS, and penicillin/streptomycin were purchased from Invitrogen Life Technologies. Abs specific for COX-2 and α-tubulin were purchased from Transduction Laboratories. Protein A/G beads, IκBα protein (aa 1–317), and Abs specific for IKKαβ phosphorylated at $Ser^{180/181}$ and p65 phosphorylated at Ser^{276} were purchased from Cell Signaling and Neuroscience. IKKαβ, p65, p50, inducible NO synthase (iNOS), and anti-mouse and anti-rabbit IgG-conjugated HRP were purchased from Santa Cruz Biotechnology. Anti-mouse and anti-rabbit IgG-conjugated alkaline phosphatases were purchased from Jackson ImmunoResearch Laboratories. pGL2-ELAM-Luc (which is under the control of one NF-κB binding site) and pBK-CMV-LacZ were kindly provided by Dr. W.-W. Lin (National Taiwan University, Taipei, Taiwan). [γ-^{32}P]ATP (6000 Ci/mmol) was purchased from Amersham Pharmacia Biotech. IL-6 was purchased from PeproTech. Anti-IL-6 Ab was purchased from eBioscience. GenePOPTER 2 was purchased from Gene Therapy System. All materials for SDS-PAGE were purchased from Bio-Rad. All other chemicals were obtained from Sigma-Aldrich.

Cell culture

The mouse macrophage cell line, RAW 264.7, was obtained from American Type Culture Collection, and cells were maintained in DMEM/Ham's F-12 nutrient mixture containing 10% FCS, 100 U/ml penicillin G, and 100 μg/ml streptomycin in a humidified 37°C incubator. After reaching confluence, cells were seeded onto either 6-cm dishes for immunoblotting or kinase assays or 12- and 24-well plates for measurement by the IL-6, PGE_2, cAMP, or κB luciferase assays.

Measurements of IL-6 and PGE_2 production

RAW 264.7 macrophages were cultured in 24-well culture plates. After reaching confluence, cells were treated with various stimulators or pretreated with specific inhibitors as indicated, followed by PGN, and then incubated in a humidified incubator at 37°C for 24 h. After incubation, the medium was removed and stored at −80°C until assay. IL-6 or PGE_2 in the medium was assayed using the IL-6 or PGE_2 enzyme immunoassay kits, respectively, according to the procedure described by the manufacturer.

Measurement of intracellular cAMP concentration

RAW 264.7 macrophages were cultured in 12-well culture plates. After reaching confluence, cells were treated with PGN (30 μg/ml) for various time intervals, or pretreated with specific inhibitors as indicated followed by PGN, and then incubated in a humidified incubator at 37°C for 6 h. After incubation, the reaction was terminated by aspiration of the medium and the addition of 0.1 N HCl for 20 min. The cells were scraped into Eppendorf tubes, and the suspensions were centrifuged; the supernatants were then neutralized with 10 N NaOH. Samples were stored at −80°C until assay. cAMP levels were assayed using the cAMP enzyme immunoassay kit according to the procedure described by the manufacturer.

Immunoblot analysis

To determine the expressions of IKKαβ phosphorylation at $Ser^{180/181}$; IKKαβ; and p65 phosphorylation at Ser^{276}, p65, iNOS, COX-2, and α-tubulin in RAW 264.7 macrophages, proteins were extracted, and Western blot analysis was performed as described previously (36). Briefly, RAW 264.7 macrophages were cultured in 6-cm dishes. After reaching confluence, cells were treated with vehicle, PGN, PGE_2, and 8-bromo-cAMP or pretreated with specific inhibitors as indicated followed by PGN. After incubation, cells were washed twice in ice-cold PBS and solubilized in extraction buffer containing 10 mM Tris (pH 7.0), 140 mM NaCl, 2 mM PMSF, 5 mM DTT, 0.5% Nonidet P-40, 0.05 mM pepstatin A, and 0.2 mM leupeptin. Samples of equal amounts of protein (100 μg) were subjected to SDS-PAGE and then transferred onto a polyvinylidine difluoride which was then incubated in 150 mM NaCl, 20 mM Tris-HCl, 0.02% Tween 20 (pH 7.4) buffer containing 5% BSA. Proteins were visualized by specific primary Abs and then incubated with HRP- or alkaline phosphatase-conjugated second Abs. Immunoreactivity was detected using ECL or nitroblue tetrazolium/5-bromo-4-chloro-3-indolyl phosphate following the manufacturer's instructions. Quantitative data were obtained using a computing densitometer with scientific imaging systems.

Immunoprecipitation and IKKαβ activity assay

RAW 264.7 cells were grown in 6-cm dishes. After reaching confluence, cells were treated with 30 μg/ml PGN for the indicated time intervals. After incubation, cells were washed twice with ice-cold PBS; lysed in 1 ml of lysis buffer containing 20 mM Tris-HCl (pH 7.5), 1 mM $MgCl_2$, 125 mM NaCl, 1% Triton X-100, 1 mM PMSF, 10 μg/ml leupeptin, 10 μg/ml aprotinin, 25 mM β-glycerophosphate, 50 mM NaF, and 100 μM sodium orthovanadate; and then centrifuged. The supernatant was immunoprecipitated with respective polyclonal Abs against IKKαβ in the presence of A/G-agarose beads overnight. The beads were washed three times with lysis buffer and twice with kinase buffer containing 20 mM HEPES (pH 7.4), 20 mM $MgCl_2$, 1 mM $NaVO_4$, and 2 mM DTT. The kinase reactions were performed by incubating immunoprecipitated beads with 20 μl of kinase buffer supplemented with 20 μM ATP and 3 μCi of [γ-^{32}P]ATP at 30°C for 30 min. To assess the IKKαβ activity, 0.5 μg of GST-IκBα protein (aa 1–317) was added to the substrate. The reaction mixtures were analyzed by 12% SDS-PAGE followed by autoradiography.

Preparation of nuclear extracts and the EMSA

RAW 264.7 macrophages were cultured in 6-cm dishes. After reaching confluence, cells were treated with 30 μg/ml PGN for indicated time intervals; then cells were scraped and collected. The cytosolic and nuclear protein fractions were separated as described previously (37). Briefly, cells were washed with ice-cold PBS and pelleted. Cell pellets were resuspended in hypotonic buffer (10 mM HEPES (pH 7.9), 10 mM KCl, 0.5 mM DTT, 10 mM aprotinin, 10 mM leupeptin, and 20 mM PMSF) for 15 min on ice, and vortexed for 10 s. Nuclei were pelleted by centrifugation at 15,000 × *g* for 1 min. Supernatants containing cytosolic proteins were collected. A pellet containing nuclei was resuspended in hypertonic buffer (20 mM HEPES (pH 7.6), 25% glycerol, 1.5 mM $MgCl_2$, 4 mM EDTA, 0.05 mM DTT, 10 mM aprotinin, 10 mM leupeptin, and 20 mM PMSF) for 30 min on ice. Supernatants containing nuclear proteins were collected by centrifugation at 15,000 × *g* for 30 min and then stored at −70°C.

A double-stranded oligonucleotide probe containing an NF-κB sequence (5′-AGTTGAGGGGACTTTCCCAGGC-3′; Promega) was purchased and end-labeled with [γ-^{32}P]ATP using T4 polynucleotide kinase. The nuclear extract (2.5–5 μg) was incubated with 1 ng of a ^{32}P-labeled NF-κB probe (50,000–75,000 cpm) in 10 μl of binding buffer containing 1 μg of poly(deoxyinosinate-deoxycytidylate), 15 mM HEPES (pH 7.6), 80 mM NaCl, 1 mM EDTA, 1 mM DTT, and 10% glycerol at 30°C for 25 min. DNA-nuclear protein complexes were separated from the DNA probe by electrophoresis on 4.5% polyacrylamide gels. Gels were vacuum dried and subjected to autoradiography with an intensifying screen at −80°C. For competition experiments, 1 ng of the labeled oligonucleotide was mixed with 50 ng of unlabeled competitor oligonucleotides before protein addition. For the supershift experiments, 4 μg of anti-p65 or anti-p50 Ab were mixed with the nuclear extract proteins.

Transfection and κB luciferase assays

For these assays, 2 × 10^5 RAW 264.7 cells were seeded onto 12-well plates, and cells were transfected the next day using GenePORTER 2 with 0.3 μg of pGL2-ELAM-Luc and 0.3 μg of pBK-CMV-LacZ. After 24 h, the medium was aspirated and replaced with fresh DMEM-Ham's F-12 containing 10% FBS and was then pretreated with specific inhibitors as indicated followed by PGN (30 μg/ml) treatment for another 24 h. Luciferase activity was determined with a luciferase assay system (Promega), and was normalized on the basis of LacZ expression. The level of induction of luciferase activity was compared as the ratio of cells with and without stimulation.

Measurement of NO concentration

NO production was assayed by measuring nitrite (a stable degradation product of NO) in the supernatant of cultured RAW 264.7 cells using the Griess reagent. Briefly, RAW 264.7 macrophages were cultured in 24-well plates. After reaching confluence, the culture medium was changed to phenol red-free DMEM. Cells were then treated with PGN (30 μg/ml) for the indicated time intervals or pretreated with specific inhibitors as indicated, followed by PGN. After incubation, the supernatant was collected, mixed with an equal volume of Griess reagent (1% sulfanilamide, 0.1% *N*-(1-naphthyl)ethylenediamine, and 2% phosphoric acid), and incubated at room temperature for 10 min. The OD measured at 550 nm in a microplate reader was used as an indication of the nitrite concentration. Sodium nitrite was used to produce a standard curve of nitrite concentration.

Statistical analysis

Results are presented as the mean ± SE from at least three independent experiments. One-way ANOVA followed by, when appropriate, Bonferroni's multiple range test was used to determine the statistical significance of the difference between means. $p < 0.05$ was considered statistically significant.

Results

PGN induces macrophage IL-6 production

Murine RAW 264.7 macrophages were chosen to investigate the signal pathways of PGN in the production of IL-6, an inflammatory response gene. Treatment with PGN (1–100 μg/ml) for 24 h induced IL-6 production in a concentration-dependent manner (Fig. 1*A*), this induction occurred in a time-dependent manner (Fig. 1*B*). After 24 h of treatment with 30 μg/ml PGN, the amount of IL-6 released had increased by ~235 ± 64% (Fig. 1*B*). To further confirm this stimulation-specific mediation by PGN without LPS contamination, polymyxin B, an LPS inhibitor, was tested. We found that polymyxin B (1 μM) completely inhibited LPS (1 μg/ml)-induced IL-6 release. However, it had no effect on PGN (30 μM)-induced IL-6 release (Fig. 1*C*).

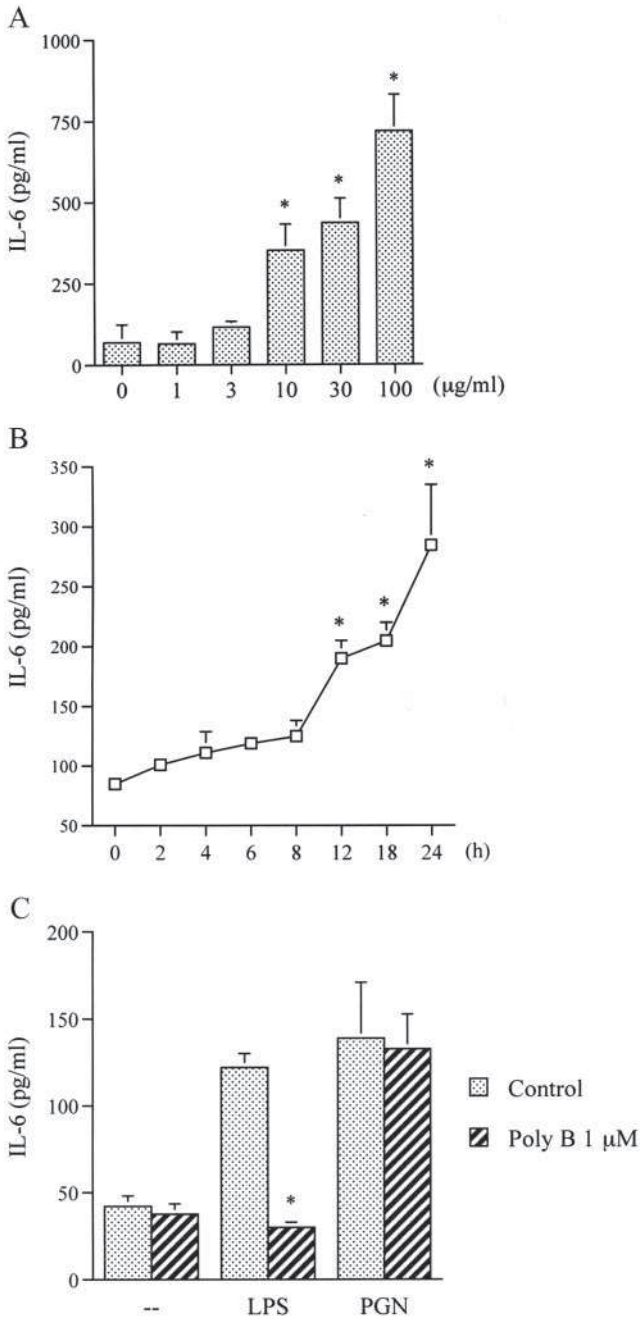

FIGURE 1. Concentration- and time-dependent increases in IL-6 production by PGN and effects of polymyxin B on LPS- and PGN-induced IL-6 production in RAW 264.7 macrophages. Cells were incubated with various concentrations of PGN for 24 h (*A*) or with 30 μg/ml PGN for 2, 4, 6, 8, 12, 18, or 24 h (*B*). Media were collected to measure IL-6. Results are expressed as the mean ± SE of four independent experiments performed in triplicate. *, $p < 0.05$ as compared with the basal level. *C*, Cells were pretreated with polymyxin B (Poly B, 1 μM) for 30 min before incubation with 1 μg/ml LPS or 30 μg/ml PGN for 24 h. Media were collected to measure IL-6. Results are expressed as the mean ± SE of three independent experiments performed in triplicate. *, $p < 0.05$ as compared with the LPS or PGN treatment groups, respectively.

Involvement of PGE_2 formation in PGN-induced IL-6 release

Our previous study showed that PGN can induce COX-2 expression in RAW 264.7 macrophages (35). Next, we further examined PGE_2 formation by PGN stimulation in RAW 264.7 macrophages. Treatment of cells with 30 μg/ml PGN for 2, 4, 6, 8, 12, 18, or 24 h induced PGE_2 formation in a time-dependent manner. PGE_2 formation increased at 2 h and peaked at 12~24 h (Fig. 2*A*). To examine whether COX-2-generated PGE_2 formation is involved in the signal transduction pathway leading to IL-6 production caused by PGN, the nonselective COX inhibitor indomethacin and the selective COX-2 inhibitor NS398 were used. Fig. 2*B* shows that PGN-induced IL-6 production was inhibited by indomethacin (10 μM) and NS398 (1 μM) by 92 ± 10% and 93 ± 7%, respectively. Furthermore, stimulation of cells with PGE_2 (0.001–1 μM) also resulted in IL-6 production in a concentration-dependent manner (Fig. 2*C*). When cells were treated with 1 μM PGE_2 for 24 h, IL-6 production increased by ~480 ± 70% (Fig. 2*C*). These results suggest that COX-2-generated PGE_2 formation is necessary for PGN-induced IL-6 release in RAW 264.7 macrophages.

Involvement of EP2 and EP4 receptors in PGN-induced IL-6 production

There are four types of EPs that have been defined and cloned, EP1, EP2, EP3, and EP4 (28). A previous study revealed that RAW 264.7 macrophages express EP2, EP3, and EP4, but not EP1, receptors (38). To identify the EP receptors involved in PGN-mediated IL-6 production, the EP2 receptor antagonist AH6809 and the EP4 receptor antagonist AH23848 were tested. As shown in Fig. 3*A*, pretreatment of RAW 264.7 macrophages with 3 μM AH6809 and 30 μM AH23848 inhibited PGN-induced IL-6 release by 49 ± 10% and 62 ± 12%, respectively. Treatment of cells with the combination of 3 μM AH6809 and 30 μM AH23848 caused a more arked inhibitory effect on the PGN-induced IL-6 release compared with each agent alone. Furthermore, treatment of RAW 264.7 macrophages with the EP2 agonist butaprost (5 μM) and the EP2/EP3/EP4 agonist misoprostol (100 nM) also resulted in IL-6 release from 75 ± 10 pg/ml to 149 ± 21 and 190 ± 20 pg/ml, respectively, whereas the EP1/EP3 agonist sulprostone (1 μM) had no effect (Fig. 3*B*). To identify the EP4-mediated effects of misoprostol, RAW 264.7 cells were treated with misoprostol in the presence of the EP2 antagonist AH6809. Treatment of cells with misoprostol in the presence of AH6809 also induced IL-6 production from 75 ± 10 pg/ml to 134 ± 23 pg/ml (Fig. 3*B*). These results suggest that PGN-induced IL-6 release may occur via activation of EP2 and EP4 receptor signaling.

Involvement of cAMP formation and PKA activation in PGN-induced IL-6 production

To identify the cAMP-dependent PKA signaling pathways involved in PGN-mediated IL-6 production, RAW 264.7 macrophages were treated with the PKA inhibitor, KT5720. Pretreatment of RAW 264.7 macrophages with KT5720 (0.01~3 μM) inhibited PGN-induced IL-6 production in a concentration-dependent manner (Fig. 4*A*). When cells were treated with 3 μM KT5720, PGN-induced IL-6 production was inhibited by 82 ± 12% ($n = 3$). Next, we directly measured cAMP formation in response to PGN. Short term treatment of cells with 30 μg/ml PGN for 5, 10, 30, and 60 min did not cause an increase in cAMP formation (data not shown). However, long term treatment of RAW 264.7 cells with PGN for 2, 4, 6, 8, or 12 h induced cAMP formation in a time-dependent manner. The cAMP formation began at 2 h, peaked at 4–8 h, and then declined at 12 h after PGN treatment (Fig. 4*B*).

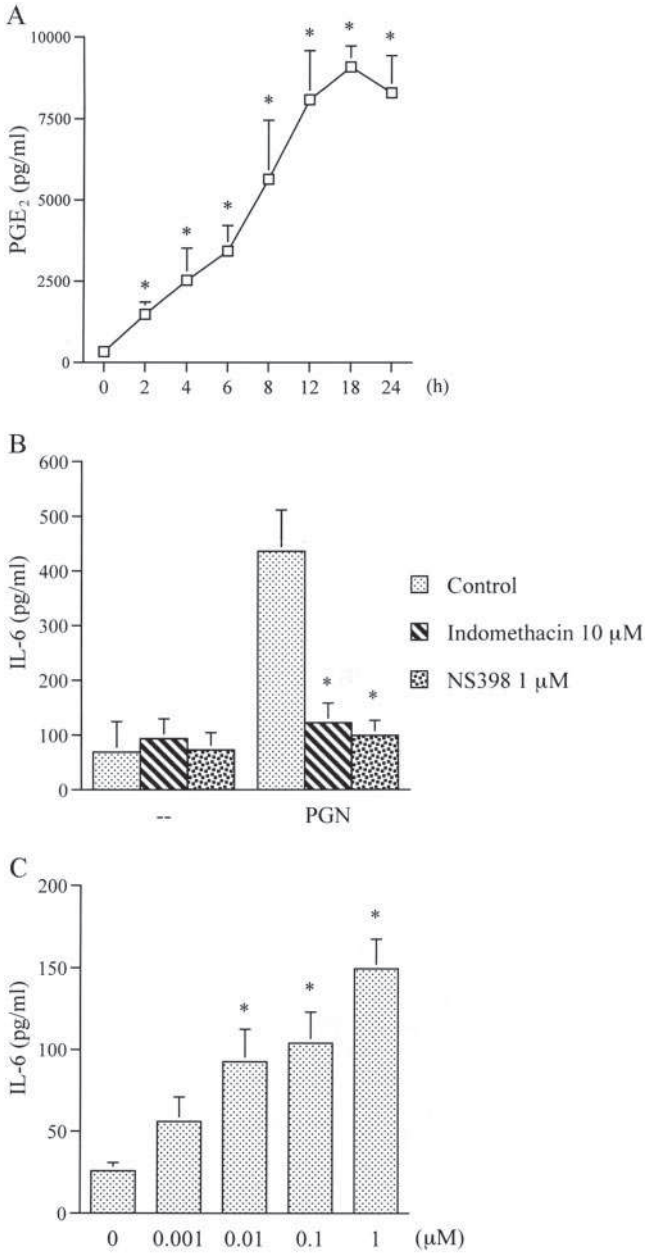

FIGURE 2. Involvement of PGE_2 formation in PGN-mediated IL-6 production in RAW 264.7 macrophages. *A*, Cells were incubated with 30 μg/ml PGN for 2, 4, 6, 8, 12, 18, or 24 h. Media were collected to measure PGE_2. Results are expressed as the mean ± SE of three independent experiments performed in triplicate. *, $p < 0.05$ as compared with the basal level. *B*, Cells were pretreated for 30 min with 10 μM indomethacin and 1 μM NS398 and then stimulated with 30 μg/ml PGN for 24 h. Media were collected to measure IL-6. Results are expressed as the mean ± SE of four independent experiments performed in triplicate. *, $p < 0.05$ as compared with the PGN treatment group. *C*, Cells were incubated with various concentrations of PGE_2 for 24 h. Media were collected to measure IL-6. Results are expressed as the mean ± SE of three independent experiments performed in triplicate. *, $p < 0.05$ as compared with the basal level.

We next examined whether PGN-induced cAMP formation occurs through COX-2-generated PGE_2 and EP2/EP4 activation. As shown in Fig. 4*C*, pretreatment of RAW 264.7 macrophages with NS398, AH6809, and AH23848 all inhibited PGN-induced cAMP formation by 90 ± 9%, 61 ± 11%, and 58 ± 15%, respectively.

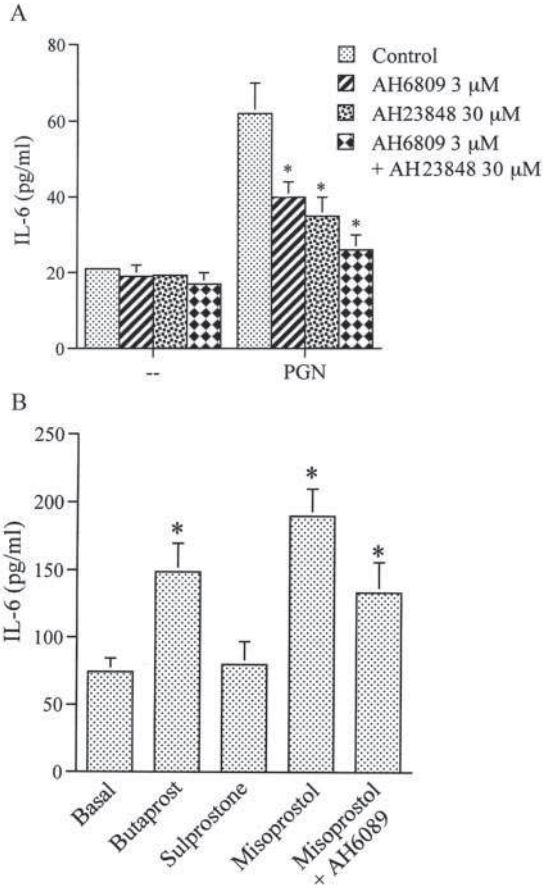

FIGURE 3. Involvement of EP2 and EP4 receptors in PGN-mediated IL-6 production in RAW 264.7 macrophages. *A*, Cells were pretreated for 30 min with 3 μM AH6809, 30 μM AH23848, or 3 μM AH6809 + 30 μM AH23848 and then stimulated with 30 μg/ml PGN for 24 h. Media were collected to measure IL-6. Results are expressed as the mean ± SE of three independent experiments performed in triplicate. *, $p < 0.05$ as compared with the PGN treatment group. *B*, Cells were incubated with 1 μM butaprost, 3 μM sulprostone, 1 μM misoprostol, or 1 μM misoprostol + 3 μM AH6089 for 24 h. Media were collected to measure IL-6. Results are expressed as the mean ± SE of three independent experiments performed in triplicate. *, $p < 0.05$ as compared with the basal level.

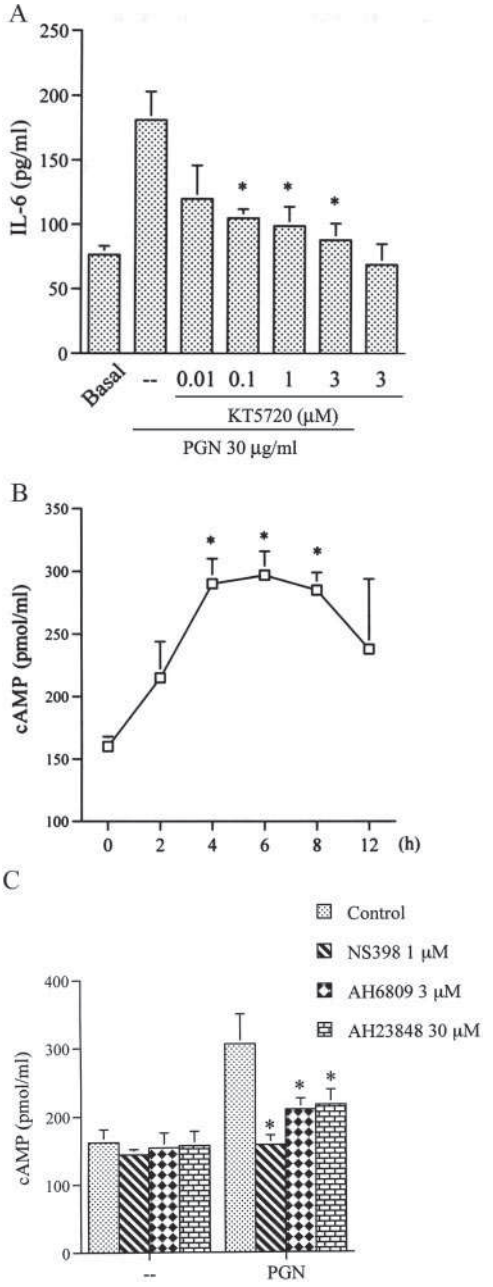

FIGURE 4. Involvement of cAMP formation and PKA activation in PGN-mediated IL-6 release in RAW 264.7 macrophages. *A*, Cells were pretreated for 30 min with various concentrations of KT5720 and then stimulated with 30 μg/ml PGN for 24 h. Media were collected to measure IL-6. Results are expressed as the mean ± SE of three independent experiments performed in triplicate. *, $p < 0.05$ as compared with the PGN treatment group. *B*, Cells were incubated with 30 μg/ml PGN for 2, 4, 6, 8, or 12 h. Cell lysates were collected to measure cAMP. Results are expressed as the mean ± SE of four independent experiments performed in triplicate. *, $p < 0.05$ as compared with the basal level. *C,* Cells were pretreated for 30 min with 1 μM NS398, 3 μM AH6809, or 30 μM AH23848 and then stimulated with 30 μg/ml PGN for 6 h. Cell lysates were collected to measure cAMP formation. Results are expressed as the mean ± SE of three independent experiments performed in triplicate. *, $p < 0.05$ as compared with the PGN treatment.

PGE_2 and PKA mediated PGN-induced IKK$\alpha\beta$ activation

We further examined whether activation of IKK$\alpha\beta$ occurs through the COX-2-generated PGE_2 and PKA signaling pathway. Stimulation of cells with 30 μg/ml PGN for 2, 4, 6, 8, or 12 h induced an increase in IKK$\alpha\beta$ phosphorylation and IKK$\alpha\beta$ activity in time-dependent manners, reaching a maximum after 6–8 h of treatment (Fig. 5). Furthermore, pretreatment of cells for 30 min with NS398 (1 μM) and KT5720 (3 μM) markedly attenuated the PGN-induced IKK$\alpha\beta$ phosphorylation by 62 ± 13% and 86 ± 15%, respectively (Fig. 6*A*). None of these inhibitors affected the basal IKK$\alpha\beta$ phosphorylation (Fig. 6*A*). In addition, treatment of RAW 264.7 macrophages with PGE_2 (1 μM) caused marked phosphorylation of IKK$\alpha\beta$, reaching maximums after 10–30 min of treatment (Fig. 6*B*, *lower*). Similarly, treatment of cells with the PKA activator, 8-bromo-cAMP (300 μM), also resulted in IKK$\alpha\beta$ phosphorylation in a time-dependent manner, with a maximum effect at 10–30 min of treatment (Fig. 6*C*). The protein level of IKK$\alpha\beta$ was not affected by PGE_2 or 8-bromo-cAMP treatment (Fig. 6, *B* and *C*, *lower*).

PGE_2 and PKA mediated PGN-induced p65 phosphorylation at Ser^{276}

Next, we further examined p65 phosphorylation at Ser^{276} by PGN stimulation in RAW 264.7 macrophages. Treatment of cells with

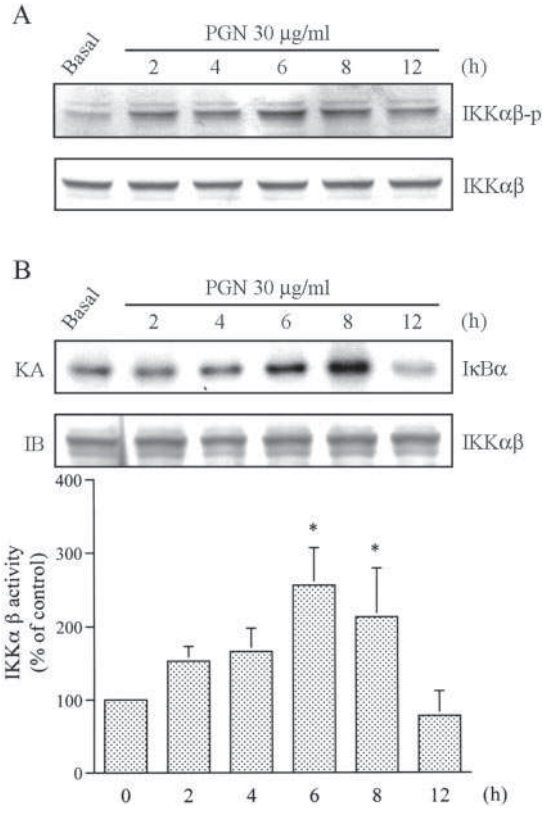

FIGURE 5. PGN induced IKK$\alpha\beta$ activation in RAW 264.7 macrophages. *A*, RAW 264.7 macrophages were treated with 30 μg/ml PGN for 2, 4, 6, 8, or 12 h, and IKK$\alpha\beta$ phosphorylation was shown by immunoblotting with an Ab specific for phosphorylated IKK$\alpha\beta$ (*upper panel*). Equal loading in each lane is shown by the similar intensities of IKK$\alpha\beta$ (*lower panel*). Typical traces are representative of three experiments with similar results. *B*, For evaluation of IKK$\alpha\beta$ activity, cell lysates were incubated with 30 μg/ml PGN for 2, 4, 6, 8, or 12 h, and then lysates were immunoprecipitated with Abs specific for IKKα and IKKβ. One set of immunoprecipitates was subjected to the kinase assay (KA) as described in *Materials and Methods* using the GST-IκBα fusion protein as a substrate (*top panel*). The other set of immunoprecipitates was subjected to 10% SDS-PAGE and analyzed by immunoblotting (IB) with an anti-IKK$\alpha\beta$ Ab (*bottom panel*). Equal amounts of the immunoprecipitated kinase complex present in each kinase assay were confirmed by immunoblotting for IKK$\alpha\beta$. Typical traces are representative of three experiments with similar results, which are presented as the mean $\pm$ SE. $*$, $p < 0.05$ as compared with the basal level.

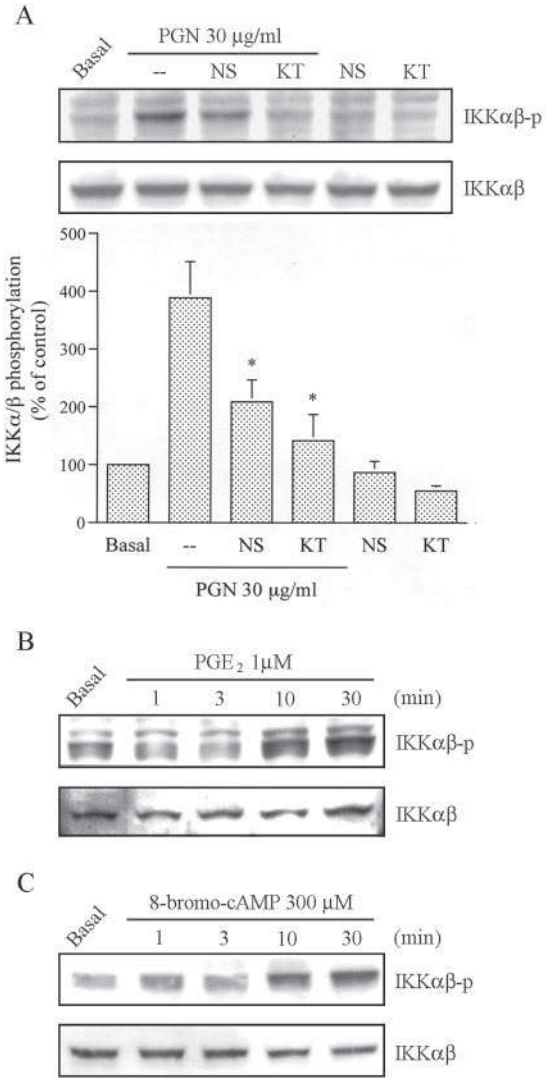

FIGURE 6. Involvement of PGE_2 formation and PKA activation in PGN-mediated IKK$\alpha\beta$ phosphorylation in RAW 264.7 macrophages. *A*, Cells were pretreated with 1 μM NS398 (NS) and 3 μM KT5720 (KT) for 30 min and then treated with 30 μg/ml PGN for 6 h. IKK$\alpha\beta$ phosphorylation was shown by immunoblotting with an Ab specific for phosphorylated IKK$\alpha\beta$ (*top panel*). Equal loading in each lane is shown by the similar intensities of IKK$\alpha\beta$ (*bottom panel*). Typical traces are representative of three experiments with similar results, presented as the mean $\pm$ SE. $*$, $p < 0.05$ as compared with the PGN treatment group. *B* and *C*, Cells were treated with 1 μM PGE_2 (*B*) or 300 μM 8-bromo-cAMP (*C*) for 1, 3, 10, or 30 min, and IKK$\alpha\beta$ phosphorylation was shown by immunoblotting with an Ab specific for phosphorylated IKK$\alpha\beta$ (*upper panel*). Equal loading in each lane is shown by the similar intensities of IKK$\alpha\beta$ (*lower panel*). Typical traces are representative of three experiments with similar results.

30 μg/ml PGN for 2, 4, 6, 8, or 12 h induced p65 phosphorylation at Ser^{276} in a time-dependent manner (Fig. 7*A*). The response began at 2 h, was sustained to 4–6 h, and then declined at 8–12 h after PGN treatment (Fig. 7*A*). We next examined whether PGN-induced p65 phosphorylation at Ser^{276} occurs through the PGE_2 and PKA signaling pathways. As shown in Fig. 7*B*, pretreatment of cells for 30 min with NS398 (1 μM) and KT5720 (3 μM) markedly attenuated PGN-induced p65 phosphorylation at Ser^{276} at 53 $\pm$ 20% and 79 $\pm$ 11%, respectively. Neither of these inhibitors affected the basal p65 protein levels (Fig. 7*B*, *lower*).

COX-2-generated PGE_2, EP2/EP4s, PKA, and IL-6 itself mediated PGN-induced NF-κB activation

To examine whether COX-2-generated PGE_2-induced NF-κB activation is required for PGN-induced IL-6 production, pretreatment of RAW 264.7 macrophages with the NF-κB inhibitor, pyrrolidine dithiocarbamate (PDTC, 50 μM), inhibited PGN- and PGE_2-induced IL-6 production by 44 $\pm$ 5% and 77 $\pm$ 14%, respectively (Fig. 8*A*). Furthermore, the time course of NF-κB activation after treatment with 30 μg/ml PGN was evaluated by a gel shift DNA binding assay. As shown in Fig. 8*B*, stimulation of cells with PGN for 10 and 30 min and 1, 2, 4, 6, 8, and 12 h resulted in a two waves of formation of the NF-κB-specific DNA-protein complex. The first wave of NF-κB activation occurred at 10–60 min of treatment and the later wave at 2–12 h of treatment. To identify the specific subunits involved in the formation of the NF-κB complex, supershift assays were performed using Abs specific for anti-p65 and anti-p50. Incubation of nuclear extracts with Abs specific for anti-p65 and anti-p50 attenuated NF-κB-specific DNA-protein

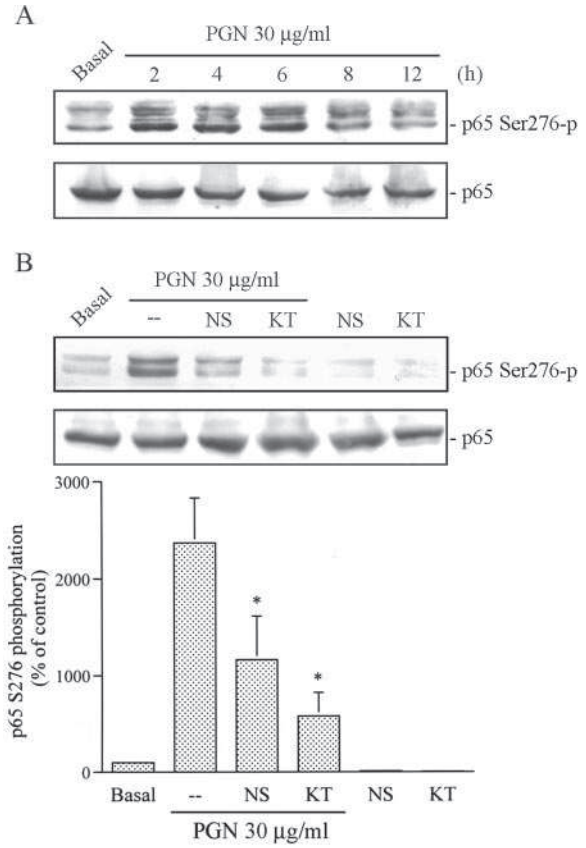

FIGURE 7. Involvement of PGE_2 formation and PKA activation in PGN-mediated p65 Ser^{276} phosphorylation (-p) in RAW 264.7 macrophages. *A,* RAW 264.7 macrophages were treated with 30 μg/ml PGN for 2, 4, 6, 8, or 12 h, and p65 phosphorylation at Ser^{276} was shown by immunoblotting with an Ab specific for phosphorylated p65 at Ser^{276} (*upper panel*). Equal loading in each lane is shown by the similar intensities of p65 (*lower panel*). Typical traces are representative of three experiments with similar results. *B*, Cells were pretreated with 1 μM NS398 (NS) and 3 μM KT5720 (KT) for 30 min and then treated with 30 μg/ml PGN for another 6 h. p65 phosphorylation at Ser^{276} was shown by immunoblotting with an Ab specific for phosphorylated p65 at Ser^{276} (*top panel*). Equal loading in each lane is shown by the similar intensities of p65 (*middle panel*). Typical traces are representative of three experiments with similar results, presented as the mean ± SE. *, $p < 0.05$ as compared with the PGN treatment group.

complex formation (Fig. 8*C*, *lanes 3* and *4*). These results indicated that the components of the NF-κB complex are p65 and p50. Formation of the NF-κB complex was completely inhibited by the 50-fold cold NF-κB consensus DNA sequence (Fig. 8*C*, *lane 5*), indicating that DNA-protein interactions are sequence specific. We further examined whether the COX-2-generated PGE_2 and PKA signaling pathway are involved in the PGN-induced activation of NF-κB in two waves. Pretreatment of cells with 1 μM NS398 or 3 μM KT5720 did not affect the first wave of NF-κB-specific DNA-protein complex formation caused by short term (30 min) treatment (Fig. 8*D*), whereas both inhibited the later wave of NF-κB activation caused by the long term (6 h) treatment of PGN (Fig. 8*E*). To directly determine NF-κB activation after PGN treatment, RAW 264.7 macrophages were transiently transfected with pGL2-ELAM-κB luciferase as an indicator of NF-κB activation. When cells were treated with 30 μg/ml PGN for 24 h, the κB luciferase activity increased by ~550 ± 62% (Fig. 9*A*). Furthermore, we found that pretreatment of cells for 30 min with 10 μM indomethacin, 1 μM NS398, and 3 μM KT5720 markedly attenuated the PGN-induced increase in κB luciferase activity by 77 ± 15%, 83 ± 14%, and 86 ± 10%, respectively (Fig. 9*A*). To test the possibility that IL-6 itself induced NF-κB activation, an anti-IL-6 Ab was used. Pretreatment of RAW 264.7 macrophages with 0.3 ng/ml anti-IL-6 Ab inhibited the PGN-induced later wave of NF-κB-specific DNA-protein complex formation (Fig. 8*E*) as well as the increase in κB luciferase activity (Fig. 9*A*). Furthermore, treatment of cells with IL-6 (1 and 10 ng/ml) also resulted in an increase in κB luciferase activity of 169 ± 17% with 10 ng/ml IL-6 treatment (Fig. 9*B*). Next, we wanted to identify whether EP2 and EP4 are involved in PGN-mediated NF-κB activation. We found that 3 μM AH6809 and 30 μM AH23848 inhibited the PGN-induced increase in κB luciferase activity by 51 ± 4% and 50 ± 6%, respectively (Fig. 9*C*). Furthermore, treatment of AH6809 and AH23848 in combination with RAW 264.7 macrophages resulted in a more marked inhibitory effect on the PGN-induced response compared with each agent alone (Fig. 9*C*). Taken together, these data suggest that COX-2-generated PGE_2, EP2/EP4, PKA, and IL-6 itself are involved in the PGN-induced later wave of NF-κB activation in RAW 264.7 macrophages.

PKC and p38 MAPK mediated PGN-induced NF-κB activation

To identify whether PKA regulates the activity of other signaling molecules that lead to NF-κB activation caused by PGN, the PKC inhibitor Ro31-8220 and the p38 MAPK inhibitor SB203580 were used. Fig. 9*D* shows that pretreatment of cells with 1 μM Ro31-8220 and 1 μM SB203580 inhibited the PGN-induced increase in κB luciferase activity by 66 ± 8% and 45 ± 8%, respectively. Furthermore, 8-bromo-cAMP, a PKA activator, which induced an increase in κB luciferase activity was also inhibited by both inhibitors by 70 ± 4% and 42 ± 5%, respectively.

NO is not involved in PGN-induced IL-6 release

Treatment with 30 μg/ml PGN for various time intervals induced iNOS expression and nitrite release in a time-dependent manner (Fig. 10, *A* and *B*). After 24 h of treatment with 30 μg/ml PGN, the nitrite release had increased by ~539 ± 131% (Fig. 10*B*). To explore whether NO might mediate PGN-induced IL-6 release, a nonselective inhibitor of NOS, L-NAME, was used. As shown in Fig. 10*C*, pretreatment of RAW 264.7 macrophages with L-NAME (100 and 300 μM) markedly inhibited the PGN-induced nitrite release by 38 ± 14% and 79 ± 9%, respectively. However, L-NAME (100 and 300 μM) did not affect PGN-induced IL-6 release (Fig. 10*D*).

Positive feedback of COX-2-generated PGE_2 in PGN-induced COX-2 expression

We further examined whether PGN-induced COX-2 expression occurs via positive feedback with the COX-2-generated PGE_2 signaling pathway. As shown in Fig. 11*A*, pretreatment of RAW 264.7 macrophages with 1 μM NS398, 10 μM indomethacin, and 1 μM KT5720 inhibited PGN-induced COX-2 expression by 53 ± 10%, 58 ± 13%, and 91 ± 5%, respectively. Furthermore, treatment of RAW 264.7 macrophages with PGE_2 (0.01–1 μM) and 8-bromo-cAMP (30–300 μM) also resulted in increases in COX-2 expression in concentration-dependent manners. When cells were treated with 1 μM PGE_2 or 300 μM 8-bromo-cAMP for 24 h, COX-2 expression increased by ~241 ± 67% or 1701 ± 243%, respectively (Fig. 11, *B* and *C*). These results suggest that PGN-induced COX-2 expression can be regulated partially through positive feedback of COX-2-generated PGE_2 and subsequently through cAMP/PKA signaling pathways.

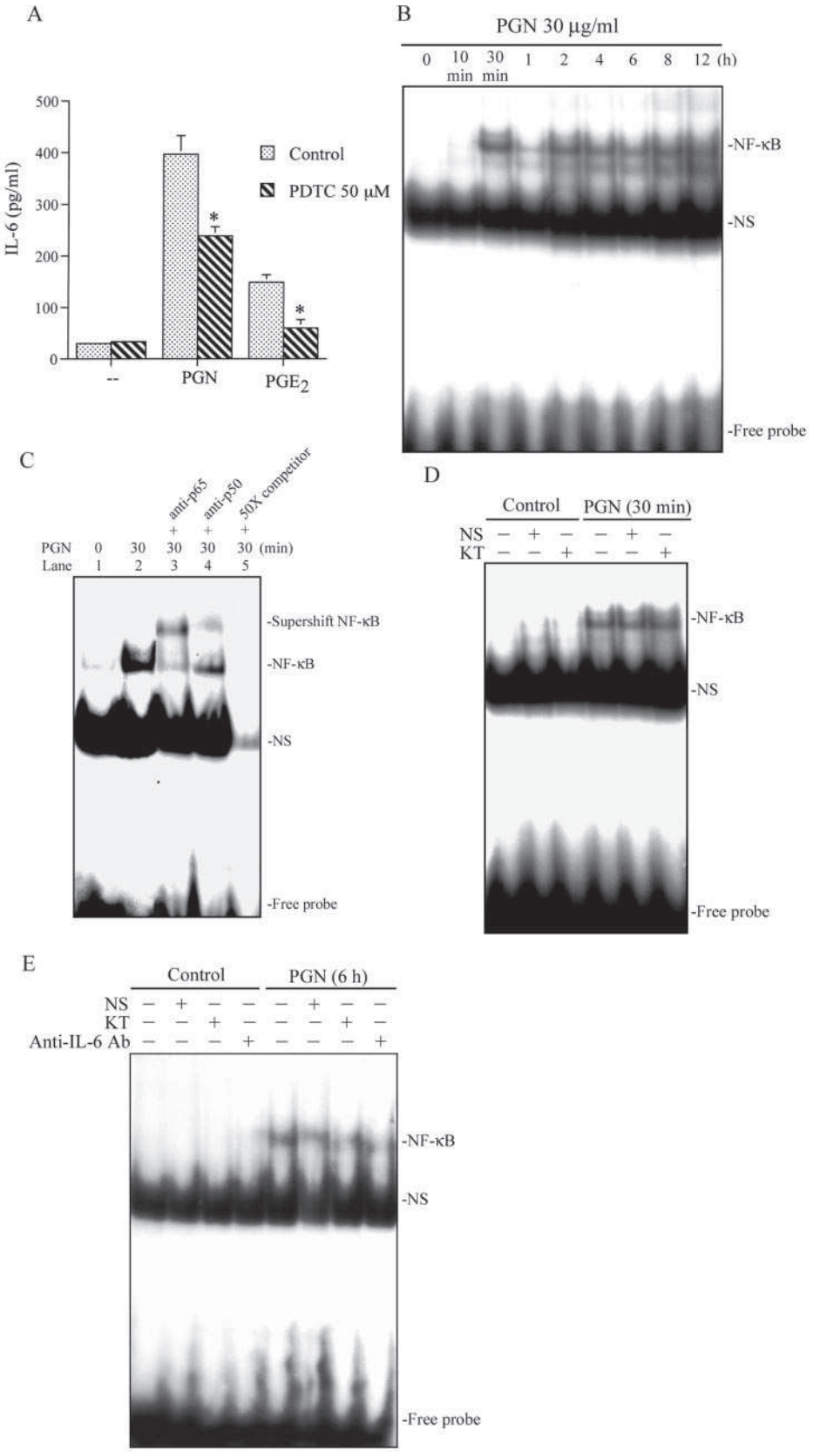

FIGURE 8. Involvement of COX-2-generated PGE_2, PKA activation, and IL-6 formation in PGN-mediated NF-κB activation in RAW 264.7 macrophages. *A*, Cells were pretreated for 30 min with 50 μM PDTC and then stimulated with 30 μg/ml PGN or 1 μM PGE_2 for 24 h. Media were collected to measure IL-6. Results are expressed as the mean ± SE of three independent experiments performed in triplicate. *, $p < 0.05$ as compared with the PGN or PGE_2 treatment group, respectively. *B*, Cells were treated with 30 μg/ml PGN for the indicated time interval. The nuclear extracts were then prepared, and NF-κB-specific DNA-protein complex formation was determined by EMSA as described in *Materials and Methods*. *Top band,* NF-κB. *C*, Cells were incubated with 30 μg/ml PGN for 30 min. The nuclear extract was prepared, and EMSA was performed as described above. *Top band,* NF-κB. Results of a competition experiment using 50-fold unlabeled NF-κB oligonucleotide (50× competitor) and a supershift experiment with 4 μg of the anti-p65 or anti-p50 Ab performed on the nuclear extract from PGN treatment are also shown. Typical traces are representative of two experiments with similar results. *D* and *E*, Cells were pretreated with 1 μM NS398 (NS), 3 μM KT5720 (KT), or 0.3 ng/ml anti-IL-6 Ab for 30 min and then stimulated with 30 μg/ml PGN for another 30 min (*D*) or 6 h (*E*) of treatment, respectively. Nuclear extracts were prepared for determination of NF-κB-specific DNA-protein complex formation by EMSA as described above. Typical traces are representative of two experiments with similar results.

Discussion

In this study, we show that PGN induces IL-6 production in RAW 264.7 macrophages by a mechanism involving COX-2 induction, PGE_2 release, and PKA activation. Several lines of evidence suggest that PGE_2 may play a vital role in IL-6 production (30–34). It has been shown that exogenous PGE_2 can stimulate IL-6 production in macrophages and astrocytes (31, 39, 40). Furthermore, it is well established that eicosanoid-producing enzymes, such as COX-2, are expressed in RAW 264.7 macrophages and are regulated by many factors, including cytokines and infectious agents

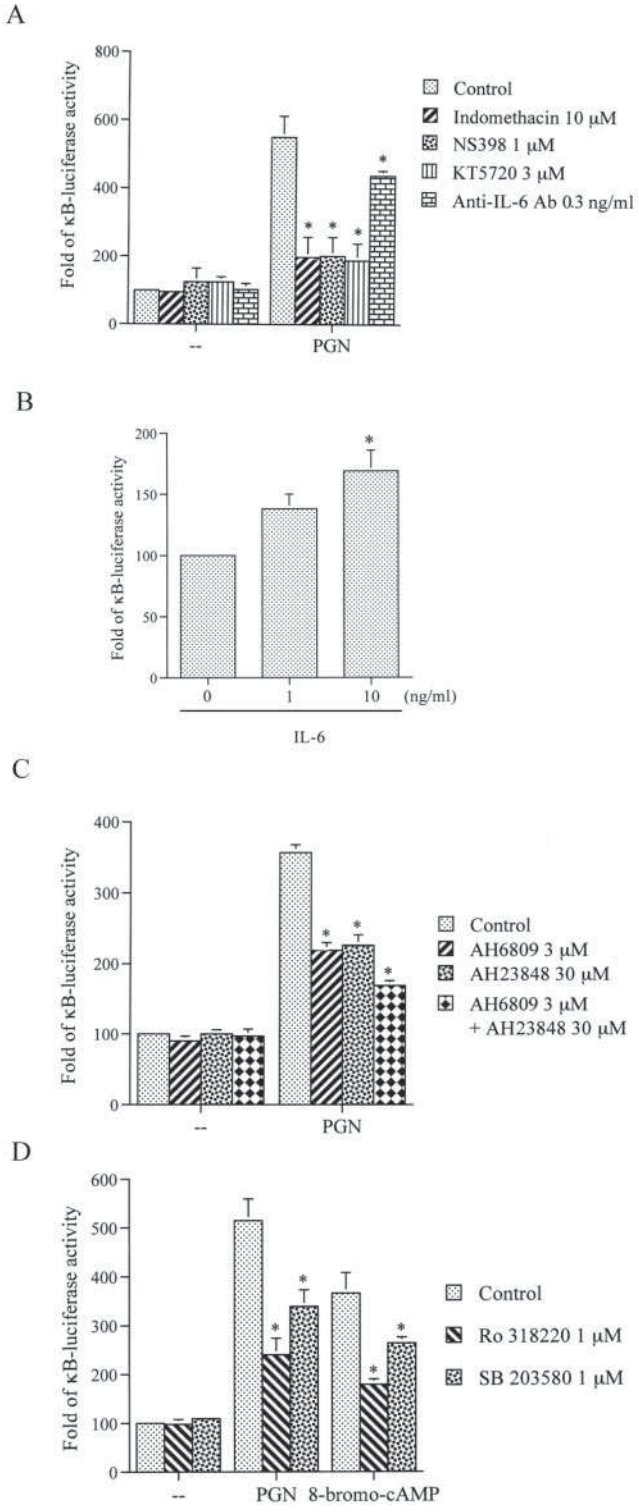

FIGURE 9. Involvement of COX-2-generated PGE_2, EP2, and EP4 receptors, IL-6 formation, p38 MAPK, and PKC activation in PGN-mediated NF-κB activation in RAW 264.7 macrophages. RAW 264.7 macrophages were transiently transfected with 0.3 μg of pGL2-ELAM-Luc and 0.3 μg of pBK-CMV-LacZ for 24 h. Cells were pretreated with 10 μM indomethacin, 1 μM NS398, 3 μM KT5720, 0.3 ng/ml anti-IL-6 Ab (*A*), 3 μM AH6809, 30 μM AH23848, 3 μM AH6809 + 30 μM AH23848 (*C*), 1 μM Ro31-8220, or 1 μM SB203580 (*D*) for 30 min and then stimulated with 30 μg/ml PGN (*A, C,* and *D*) or 300 nM 8-bromo-cAMP (*D*) for another 24 h. Luciferase activities were determined as described in *Materials and Methods*. The level of induction of luciferase activity was compared with that of cells without PGN (*A, C,* and *D*) or 8-bromo-cAMP (*D*) treatment. Data represent the mean ± SE of three experiments performed in duplicate. ∗, $p < 0.05$ as compared with the PGN (*A, C,* and *D*) or 8-bromo-cAMP (*D*) treatment group, respectively. *B*, RAW 264.7 macrophages were transiently transfected with 0.3 μg of pGL2-ELAM-Luc and 0.3 μg of pBK-CMV-LacZ for 24 h. Cells were stimulated with IL-6 (1–10 ng/ml) for another 24 h. Luciferase activities were determined as described above. The level of induction of luciferase activity was compared with that of cells without IL-6 treatment. Data represent the mean ± SE of three experiments performed in duplicate. ∗, $p < 0.05$ as compared with the basal level.

(35, 41, 42). Furthermore, COX-2 is thought to contribute to the generation of PGs at sites of inflammation (27). Because PGN has been shown to stimulate COX-2 protein expression after 2 h of treatment (35), we hypothesized that COX-2 products may be involved in mediating the PGN-induced increase in IL-6 production. Our study has revealed that PGN induced PGE_2 formation in a time-dependent manner. The respective increases after 2, 4, 6, 8, 12, 18, and 24 h of treatment were 3-, 7-, 9-, 16-, 23-, 26-, and 24-fold of the basal level, paralleling the increase in COX-2 expression stimulated by PGN (35). We also found that PGE_2 added to the culture medium increases IL-6 production and that the nonselective COX inhibitor indomethacin and the selective COX-2 inhibitor NS398 blocked PGN-induced IL-6 production. These results indicate that COX-2-generated PGE_2 plays a critical role in PGN-stimulated IL-6 production. Furthermore, we found that PGN induces iNOS expression and nitrite release and that the nonselective NOS inhibitor, L-NAME, did not inhibit PGN-induced IL-6 production, suggesting that iNOS expression and NO formation are not involved in the signaling pathway of PGN-induced IL-6 production. These findings support those from another study on LPS (32), a cell wall component of Gram-negative bacteria, in J774.2 macrophages. We also found that treatment of RAW 264.7 cells with PGE_2 and the PKA activator 8-bromo-cAMP resulted in increases in COX-2 expression and that indomethacin, NS398, and the PKA inhibitor KT5720 blocked PGN-induced COX-2 expression. These results suggest that PGN-induced COX-2 expression may be partially regulated through positive feedback of COX-2-generated PGE_2 and subsequently through cAMP/PKA signaling pathways.

The action of PGE_2 occurs via four different transmembrane receptors, namely EP1, EP2, EP3, and EP4 (28). Previous studies demonstrated that RAW 264.7 macrophages express EP2, EP3, and EP4, but not EP1, receptors (38). We found that the EP2 antagonist AH6809 and the EP4 antagonist AH23848 markedly inhibited PGN-induced IL-6 production. The combination of AH6809 and AH23848 showed a more marked inhibitory effect. Although AH23848 is also a thromboxane A_2 receptor (TP) antagonist, RAW 264.7 macrophages do not express the TP (38). Therefore, we ruled out the possibility that the inhibitory effect of AH23848 on PGN-induced IL-6 release occurs via the TP. Previous studies have indicated that sulprostone, butaprost, and misoprostol are agonists for EP1/EP3, EP2, and EP2/EP3/EP4, respectively (43, 44). In this study, we found that butaprost, misoprostol, and misoprostol in the presence of the EP2 antagonist AH6809 resulted in IL-6 release, whereas sulprostone did not. These results suggest that PGN-stimulated IL-6 production is mediated via the EP2 and EP4 receptors. EP2 and EP4 are G-protein-coupled receptors that activate adenylyl cyclase upon ligand binding and result in increased cAMP levels and activation of PKA (29). In this study, we found that PGN induced cAMP formation and that NS398, AH6809, and AH23848 inhibited PGN-induced cAMP formation. Furthermore, the specific PKA inhibitor suppressed PGN-induced IL-6 production. The increase in cAMP formation was approximately parallel to the levels of endogenously produced

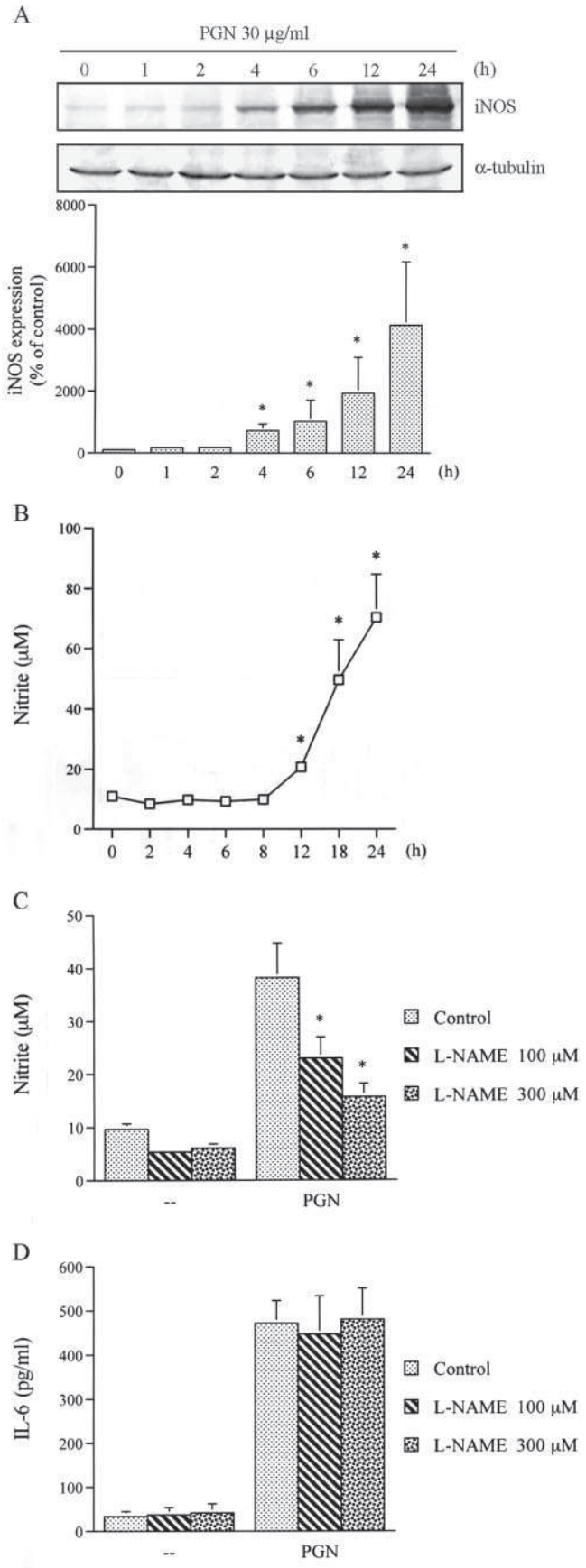

FIGURE 10. NO is not involved in PGN-mediated IL-6 production in RAW 264.7 macrophages. *A*, Cells were incubated with 30 μg/ml PGN for the indicated time intervals and then immunodetected using specific Abs against iNOS or α-tubulin as described in *Materials and Methods*. Data are representative of three independent experiments that gave essentially identical results. The extents of iNOS and α-tubulin protein expressions were quantitated using a densitometer with scientific imaging systems. The relative level was calculated as a percentage of the control level. Results are expressed as the mean ± SE of three independent experiments performed in triplicate. *, $p < 0.05$ as compared with the control group. Equal loading in each lane is demonstrated by similar intensities of α-tubulin. *B*, Cells were incubated with 30 μg/ml PGN for the indicated time intervals. Media were collected to measure nitrite release. Results are expressed as the mean ± SE of three independent experiments performed in triplicate. *, $p < 0.05$ as compared with the control group. *C* and *D*, Cells were pretreated for 30 min with vehicle or L-NAME (100 and 300 μM) and then stimulated with 30 μg/ml PGN for 24 h. Media were collected to measure of nitrite (*C*) and IL-6 (*D*), respectively. Results are expressed as the mean ± SE of four independent experiments performed in triplicate. *, $p < 0.05$ as compared with the PGN treatment group.

PGE_2 stimulated by PGN. These results suggest that COX-2-generated PGE_2 acts as an autocrine/paracrine factor for stimulating PGN-induced IL-6 production via the EP2/EP4 receptor-mediated cAMP/PKA signaling pathways. This suggestion is further supported by previous reports that LPS induces an increase in cAMP levels through PGE_2 formation in peritoneal macrophages and RAW 264.7 macrophages (45, 46). A previous report also indicated that in cultured Caco-2 cells, the cAMP-dependent PKA signaling pathway is involved in IL-1β-induced IL-6 production (47).

In mice and humans, the IL-6 promoter has many transcription factors including NF-κB in the 5′ region of the *IL-6* gene (11, 12). Several studies have demonstrated that NF-κB plays a vital role in mediating the up-regulation of IL-6 protein induced by several inflammatory mediators (48, 49). We found that the NF-κB inhibitor PDTC inhibited PGN- and PGE_2-induced IL-6 production, suggesting that PGE_2-dependent NF-κB activation is required for PGN-induced IL-6 production. Short term (5–60 min) treatment of cells with PGN did not cause an increase in cAMP formation, whereas long term (2–12 h) treatment of cells induced cAMP formation, with a maximum effect at 4–8 h after PGN treatment. Furthermore, stimulation of cells with PGN resulted in a two waves of formation of the NF-κB-specific DNA-protein complex. The first wave of NF-κB activation occurred at 10–60 min of treatment, whereas the later wave occurred at 2–12 h of treatment. We also found that a specific COX-2 inhibitor and a PKA inhibitor inhibited the PGN-induced later wave of NF-κB-specific DNA-protein complex formation, but not the first wave of NF-κB activation. These results suggest that PGN-induced IL-6 production requires two separate activation steps for NF-κB: the first wave of NF-κB activation may be PGE_2/cAMP-independent; whereas the later wave of NF-κB activation may be PGE_2/cAMP dependent.

It has been shown that the cAMP/PKA pathway is involved in LPS-induced NF-κB activation in RAW 264.7 macrophages (46). PKA was found to mediate NF-κB activation through the IKK$\alpha\beta$ complex in J774.2 macrophages (50). In the present study, we found that the PGN-mediated increase in IKK$\alpha\beta$ activity is a delayed event. The respective increases after 2, 4, 6, and 8 h of treatment were 0.5-, 0.6-, 2.5-, and 2.1-fold of the basal level, with the maximum effect at 6–8 h treatment, paralleling the increase in cAMP formation. The later wave activation of DNA-protein complex formation caused by PGN showed an increase after 2 h of treatment and a maximal level at 8–12 h of treatment; this occurred downstream of IKK$\alpha\beta$ activation. We also found that a specific COX-2 inhibitor and a PKA inhibitor inhibit the PGN-induced increase in IKK$\alpha\beta$ activation and κB luciferase activity. Furthermore, exogenous PGE_2 and the direct PKA activator 8-bromo-cAMP also cause IKK$\alpha\beta$ activation or an increase in κB luciferase activity. These results indicate that IKK$\alpha\beta$-dependent

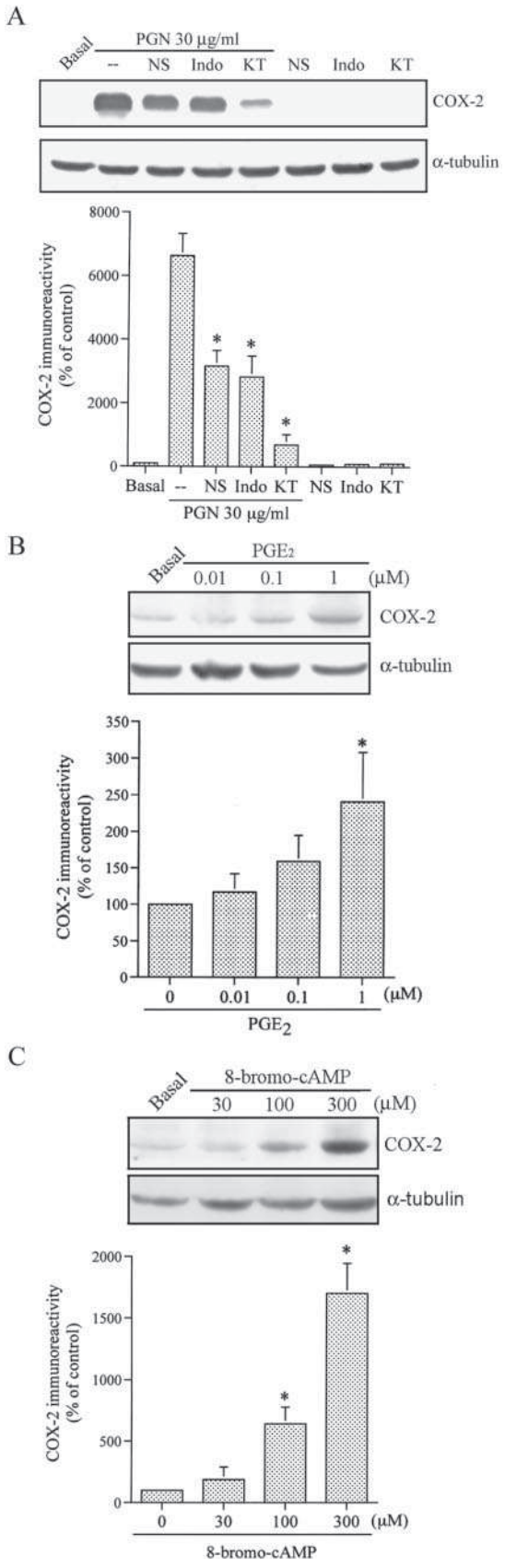

FIGURE 11. Positive feedback of COX-2-generated PGE_2 involved in PGN-mediated COX-2 expression in RAW 264.7 macrophages. *A*, Cells were pretreated with 1 μM NS398 (NS), 10 μM indomethacin (Indo), and 3 μM KT5720 (KT) for 30 min followed by stimulation with 30 μg/ml PGN for another 24 h, and COX-2 expression was determined by immunoblotting with an Ab specific for COX-2. Equal loading in each lane is demonstrated by the similar intensities of α-tubulin. Typical traces are representative of three experiments with similar results, which are presented as the mean $\pm$ SE. $*$, $p < 0.05$ as compared with PGN treatment. In *B* and *C*, cells were incubated with PGE_2 (0.01–1 μM) (*B*) or 8-bromo-cAMP (30–300 μM) (*C*) for 24 h, and then COX-2 or α-tubulin protein levels were determined. Equal loading in each lane is shown by the similar intensities of α-tubulin. Traces represent results from three independent experiments, presented as the mean $\pm$ SE. $*$, $p < 0.05$ as compared with the control group.

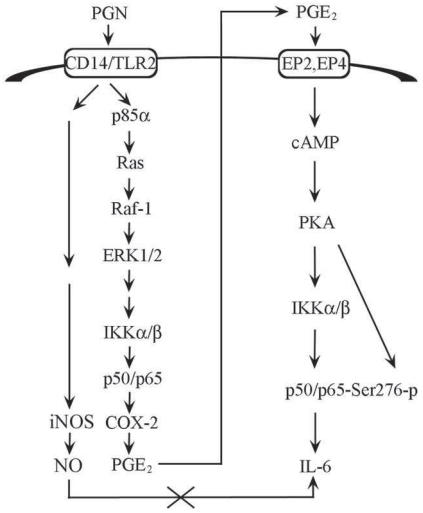

FIGURE 12. Schematic summary of signal transduction by PGN induction of macrophage IL-6 production in RAW 264.7 macrophages. PGN might activate the Ras/Raf-1/ERK pathway through recruitment of Ras and p85α to TLR2 to mediate an increase in IKK$\alpha\beta$ activity and p50/p65 (NF-κB) activation, which lead to COX-2 expression and PGE_2 release. PGN-induced PGE_2 release result in activation of the EP2 and EP4 receptors and the cAMP/PKA pathway, which in turn increase IKK$\alpha\beta$ activity, p65 phosphorylation at Ser^{276}, and NF-κB activation, and finally induce IL-6 production in RAW 264.7 macrophages. However, PGN-induced NO release is not involved in the signaling pathway of PGN-induced IL-6 production.

NF-κB activation occurs downstream of the signaling pathway of COX-2-generated PGE_2 and PKA activation stimulated by PGN. Moreover, we also showed that the EP2 antagonist, AH6809, and the EP4 receptor antagonist, AH23848, inhibited the PGN-induced increase in κB luciferase activity. The combination of AH6809 and AH23848 resulted in a more marked inhibitory effect in the PGN-induced increase in κB luciferase activity. These results suggest that COX-2-generated PGE_2 induced by PGN occurs via EP2 and EP4 receptor activation by mediating NF-κB activation. Previous studies have also shown that IL-6 induces NF-κB activation in intestinal epithelial cells (51). Therefore, it is possible that IL-6 production is involved in PGN-induced NF-κB activation. In the present study, we found that IL-6 caused an increase in κB luciferase activity and that the anti-IL-6 Ab inhibited the PGN-induced later wave of NF-κB-specific DNA-protein complex formation and an increase in κB luciferase activity. These results suggest that IL-6 production also acts as an autocrine/paracrine factor for PGN-induced NF-κB activation. In this study, we also found that a PKC inhibitor (Ro31-8220) and a p38 MAPK inhibitor (SB203580) inhibited the PGN- and 8-bromo-cAMP-induced increase in κB luciferase activity, suggesting that PKA regulates the activities of PKC and p38 MAPK that leads to NF-κB activation caused by PGN. This suggestion is further supported by a previous report that

PKA induces NF-κB activation via the PKC and p38 MAPK signaling pathway in J774.2 macrophages (50).

Recent studies have suggested that PKA may be involved in events leading to enhanced phosphorylation of the p65 subunit of NF-κB and the subsequent enhanced transactivation potential of NF-κB once it is bound to its consensus sequence (21, 52). In this study, we found that PGN causes p65 phosphorylation at Ser^{276} in a time-dependent manner. The maximum occurred after 6 h of treatment, and this effect was parallel to cAMP formation, IKKαβ activation, and NF-κB activation. Furthermore, a specific COX-2 inhibitor (NS398) and a PKA inhibitor (KT5720) inhibited PGN-stimulated p65 phosphorylation at Ser^{276}. These results suggest that p65 phosphorylation also occurs downstream of COX-2-generated PGE_2 and PKA activation in the PGN-mediated signaling pathway.

In conclusion, the findings of our study for the first time show that PGN-induced IL-6 production involves COX-2-generated PGE_2, EP2, and EP4 receptor activation; intracellular cAMP formation; and the activations of PKA, PKC, p38 MAPK, IKKαβ, p65 phosphorylation, and NF-κB. PGN-induced COX-2 expression may be partially regulated through positive feedback by COX-2-generated PGE_2 formation. However, PGN-induced iNOS expression and nitrite release were not involved in the signaling pathway of PGN-induced IL-6 production. Fig. 12 is a schematic representation of the signaling pathway of PGN-induced IL-6 production in RAW 264.7 macrophages. By understanding these signal transduction pathways, we can design therapeutic strategies to reduce inflammation caused by Gram-positive organisms.

Acknowledgments

We thank Dr. Wan-Wan Lin for the gifts of the pGL2-ELAM-Luc and pBK-CMV-LacZ plasmids.

Disclosures

The authors have no financial conflict of interest.

References

1. Medzhitov, R., and C. A. Janeway, Jr. 1998. An ancient system of host defense. *Curr. Opin. Immunol.* 10: 12–15.
2. Hoffmann, J. A., F. C. Kafatos, C. A. Janeway, and R. A. Ezekowitz. 1999. Phylogenetic perspectives in innate immunity. *Science* 284: 1313–1318.
3. Dziarski, R., A. J. Ulmer, and D. Gupta. 2000. Interactions of CD14 with components of Gram-positive bacteria. *Chem. Immunol.* 74: 83–107.
4. Bone, R. C. 1994. Gram-positive organisms and sepsis. *Arch. Intern. Med.* 154: 26–34.
5. Ulevitch, R. J., and P. S. Tobias. 1995. Receptor-dependent mechanisms of cell stimulation by bacterial endotoxin. *Annu. Rev. Immunol.* 13: 437–457.
6. Graeve, L., M. Baumann, and P. C. Heinrich. 1993. Interleukin-6 in autoimmune disease: role of IL-6 in physiology and pathology of the immune defense. *Clin. Invest.* 71: 664–671.
7. Grimble, R. F. 1998. Nutritional modulation of cytokine biology. *Nutrition* 14: 634–640.
8. Jones, S. A. 2005. Directing transition from innate to acquired immunity: defining a role for IL-6. *J. Immunol.* 175: 3463–3468.
9. Yokota, K., T. Miyazaki, M. Hirano, Y. Akiyama, and T. Mimura. 2006. Simvastatin inhibits production of interleukin 6 (IL-6) and IL-8 and cell proliferation induced by tumor necrosis factor-α in fibroblast-like synoviocytes from patients with rheumatoid arthritis. *J. Rheumatol.* 33: 463–471.
10. Hirano, T. 1992 Interleukin-6 and its relation to inflammation and disease. *Clin. Immunol. Immunopathol.* 62:S60–S65.
11. Grassl, C., B. Luckow, D. Schlondorff, and U. Dendorfer. 1999. Transcriptional regulation of the interleukin-6 gene in mesangial cells. *J. Am. Soc. Nephrol.* 10: 1466–1477.
12. Matsusaka, T., K. Fujikawa, Y. Nishio, N. Mukaida, K. Matsushima, T. Kishimoto, and S. Akira. 1993. Transcription factors NF-IL6 and NF-κB synergistically activate transcription of the inflammatory cytokines, interleukin 6 and interleukin 8. *Proc. Natl. Acad. Sci. USA* 90: 10193–10197.
13. Baldwin, A. S., Jr. 1996. The NF-κB and IκB proteins: new discoveries and insights. *Annu. Rev. Immunol.* 14: 649–683.
14. Thompson, J. E., R. J. Phillips, H. Erdjument-Bromage, P. Tempst, and S. Ghosh. 1995. IκB-β regulates the persistent response in a biphasic activation of NF-κB. *Cell* 80: 573–582.
15. DiDonato, J. A., M. Hayakawa, D. M. Rothwarf, E. Zandi, and M. Karin. 1997. A cytokine-responsive IκB kinase that activates the transcription factor NF-κB. *Nature* 388: 548–554.
16. Maniatis, T. 1997. Catalysis by a multiprotein IκB kinase complex. *Science* 278: 818–819.
17. Woronicz, J. D., X. Gao, Z. Cao, M. Rothe, and D. V. Goeddel. 1997. IκB kinase-β: NF-κB activation and complex formation with IκB kinase-α and NIK. *Science* 278: 866–869.
18. Chen, Z., J. Hagler, V. J. Palombella, F. Melandri, D. Scherer, D. Ballard, and T. Maniatis. 1995. Signal-induced site-specific phosphorylation targets IκBα to the ubiquitin-proteasome pathway. *Genes Dev.* 9: 1586–1597.
19. Vanden Berghe, W., S. Plaisance, E. Boone, K. De Bosscher, M. L. Schmitz, W. Fiers, and G. Haegeman. 1998. p38 and extracellular signal-regulated kinase mitogen-activated protein kinase pathways are required for nuclear factor-κB p65 transactivation mediated by tumor necrosis factor. *J. Biol. Chem.* 273: 3285–3290.
20. Bergmann, M., L. Hart, M. Lindsay, P. J. Barnes, and R. Newton. 1998. IκBα degradation and nuclear factor-κB DNA binding are insufficient for interleukin-1β and tumor necrosis factor-α-induced κB-dependent transcription: requirement for an additional activation pathway. *J. Biol. Chem.* 273: 6607–6610.
21. Zhong, H., R. E. Voll, and S. Ghosh. 1998. Phosphorylation of NF-κB p65 by PKA stimulates transcriptional activity by promoting a novel bivalent interaction with the coactivator CBP/p300. *Mol. Cell* 1: 661–671.
22. Wang, D., and A. S. Baldwin, Jr. 1998. Activation of nuclear factor-κB-dependent transcription by tumor necrosis factor-α is mediated through phosphorylation of RelA/p65 on serine 529. *J. Biol. Chem.* 273: 29411–29416.
23. Perkins, N. D., L. K. Felzien, J. C. Betts, K. Leung, D. H. Beach, and G. J. Nabel. 1997. Regulation of NF-κB by cyclin-dependent kinases associated with the p300 coactivator. *Science* 275: 523–527.
24. Smith, W. L., D. L. DeWitt, and R. M. Garavito. 2000. Cyclooxygenases: structural, cellular, and molecular biology. *Annu. Rev. Biochem.* 69: 145–182.
25. Murakami, M., R. Matsumoto, K. F. Austen, and J. P. Arm. 1994. Prostaglandin endoperoxide synthase-1 and -2 couple to different transmembrane stimuli to generate prostaglandin D_2 in mouse bone marrow-derived mast cells. *J. Biol. Chem.* 269: 22269–22275.
26. DeWitt, D., and W. L. Smith. 1995. Yes, but do they still get headaches? *Cell* 83: 345–348.
27. Otto, J. C., and W. L. Smith. 1995. Prostaglandin endoperoxide synthases-1 and -2. *J. Lipid Mediat. Cell. Signal.* 12: 139–156.
28. Narumiya, S., and G. A. FitzGerald. 2001. Genetic and pharmacological analysis of prostanoid receptor function. *J. Clin. Invest.* 108: 25–30.
29. Bos, C. L., D. J. Richel, T. Ritsema, M. P. Peppelenbosch, and H. H. Versteeg. 2004. Prostanoids and prostanoid receptors in signal transduction. *Int. J. Biochem. Cell Biol.* 36: 1187–1205.
30. Ogle, C. K., X. Guo, K. Szczur, S. Hartmann, and J. D. Ogle. 1994. Production of tumor necrosis factor, interleukin-6 and prostaglandin E_2 by LPS-stimulated rat bone marrow macrophages after thermal injury: effect of indomethacin. *Inflammation* 18: 175–185.
31. Hinson, R. M., J. A. Williams, and E. Shacter. 1996. Elevated interleukin 6 is induced by prostaglandin E_2 in a murine model of inflammation: possible role of cyclooxygenase-2. *Proc. Natl. Acad. Sci. USA* 93: 4885–4890.
32. Chen, B. C., and W. W. Lin. 1999. Potentiation of lipopolysaccharide-induced IL-6 release by uridine triphosphate in macrophages: cross-interaction with cyclooxygenase-2-dependent prostaglandin E_2 production. *J. Biomed. Sci.* 6: 425–432.
33. Spangelo, B. L., P. C. Isakson, and R. M. MacLeod. 1990. Production of interleukin-6 by anterior pituitary cells is stimulated by increased intracellular adenosine 3′,5′-monophosphate and vasoactive intestinal peptide. *Endocrinology* 127: 403–409.
34. Anderson, G. D., S. D. Hauser, K. L. McGarity, M. E. Bremer, P. C. Isakson, and S. A. Gregory. 1996. Selective inhibition of cyclooxygenase (COX)-2 reverses inflammation and expression of COX-2 and interleukin 6 in rat adjuvant arthritis. *J. Clin. Invest.* 97: 2672–2679.
35. Chen, B. C., Y. S. Chang, J. C. Kang, M. J. Hsu, J. R. Sheu, T. L. Chen, C. M. Teng, and C. H. Lin. 2004. Peptidoglycan induces nuclear factor-κB activation and cyclooxygenase-2 expression via Ras, Raf-1, and ERK in RAW 264.7 macrophages. *J. Biol. Chem.* 279: 20889–20897.
36. Lin, C. H., I. H. Kuan, H. M. Lee, W. S. Lee, J. R. Sheu, Y. S. Ho, C. H. Wang, and H. P. Kuo. 2001. Induction of cyclooxygenase-2 protein by lipoteichoic acid from *Staphylococcus aureus* in human pulmonary epithelial cells: involvement of a nuclear factor-κB-dependent pathway. *Br. J. Pharmacol.* 134: 543–552.
37. Chen, C. C., J. K. Wang, W. C. Chen, and S. B. Lin. 1998. Protein kinase Cη mediates lipopolysaccharide-induced nitric-oxide synthase expression in primary astrocytes. *J. Biol. Chem.* 273: 19424–19430.
38. Arakawa, T., O. Laneuville, C. A. Miller, K. M. Lakkides, B. A. Wingerd, D. L. DeWitt, and W. L. Smith. 1996. Prostanoid receptors of murine NIH 3T3 and RAW 264.7 cells: structure and expression of the murine prostaglandin EP4 receptor gene. *J. Biol. Chem.* 271: 29569–29575.
39. Martin, C. A., and M. E. Dorf. 1990. Interleukin-6 production by murine macrophage cell lines P388D1 and J774A. 1. Stimulation requirements and kinetics. *Cell. Immunol.* 128: 555–568.
40. Fiebich, B. L., S. Schleicher, O. Spleiss, M. Czygan, and M. Hull. 2001. Mechanisms of prostaglandin E_2-induced interleukin-6 release in astrocytes: possible involvement of EP4-like receptors, p38 mitogen-activated protein kinase and protein kinase C. *J. Neurochem.* 79: 950–958.
41. Chiang, L. L., C. T. Kuo, C. H. Wang, T. F. Chen, Y. S. Ho, H. P. Kuo, and C. H. Lin. 2003. Involvement of nuclear factor-κB in lipoteichoic acid-induced

cyclooxygenase-2 expression in RAW 264.7 macrophages. *J. Pharm. Pharmacol.* 55: 115–123.

42. Huang, Z. F., J. B. Massey, and D. P. Via. 2000. Differential regulation of cyclooxygenase-2 (COX-2) mRNA stability by interleukin-1β (IL-1β) and tumor necrosis factor-α (TNF-α) in human in vitro differentiated macrophages. *Biochem. Pharmacol.* 59: 187–194.
43. Hata, A. N., and R. M. Breyer. 2004. Pharmacology and signaling of prostaglandin receptors: multiple roles in inflammation and immune modulation. *Pharmacol. Ther.* 103: 147–166.
44. Zeng, L., S. An, and E. J. Goetzl. 1998 EP4/EP2 receptor-specific prostaglandin E_2 regulation of interleukin-6 generation by human HSB.2 early T cells. *J. Pharmacol. Exp. Ther.* 286: 1420–1426.
45. Raddassi, K., J. F. Petit, and G. Lemaire. 1993. LPS-induced activation of primed murine peritoneal macrophages is modulated by prostaglandins and cyclic nucleotides. *Cell Immunol.* 149: 50–64.
46. Chen, C. C., K. T. Chiu, Y. T. Sun, and W. C. Chen. 1999. Role of the cyclic AMP-protein kinase A pathway in lipopolysaccharide-induced nitric oxide synthase expression in RAW 264.7 macrophages: involvement of cyclooxygenase-2. *J. Biol. Chem.* 274: 31559–31564.
47. Hershko, D. D., B. W. Robb, G. Luo, and P. O. Hasselgren. 2002. Multiple transcription factors regulating the IL-6 gene are activated by cAMP in cultured Caco-2 cells. *Am. J. Physiol.* 283: R1140–R1148.
48. Skurk, T., V. van Harmelen, and H. Hauner. 2004. Angiotensin II stimulates the release of interleukin-6 and interleukin-8 from cultured human adipocytes by activation of NF-κB. *Arterioscler. Thromb. Vasc. Biol.* 24: 1199–1203.
49. Fan, Z., B. Bau, H. Yang, and T. Aigner. 2004. IL-1β induction of IL-6 and LIF in normal articular human chondrocytes involves the ERK, p38 and NFκB signaling pathways. *Cytokine* 28: 17–24.
50. Chio, C. C., Y. H. Chang, Y. W. Hsu, K. H. Chi, and W. W. Lin. 2004. PKA-dependent activation of PKC, p38 MAPK and IKK in macrophage: implication in the induction of inducible nitric oxide synthase and interleukin-6 by dibutyryl cAMP. *Cell. Signal.* 16: 565–575.
51. Wang, L., B. Walia, J. Evans, A. T. Gewirtz, D. Merlin, and S. V. Sitaraman. 2003. IL-6 induces NF-κB activation in the intestinal epithelia. *J. Immunol.* 171: 3194–3201.
52. Bird, T. A., K. Schooley, S. K. Dower, H. Hagen, and G. D. Virca. 1997. Activation of nuclear transcription factor NF-κB by interleukin-1 is accompanied by casein kinase II-mediated phosphorylation of the p65 subunit. *J. Biol. Chem.* 272: 32606–32612.

THE JOURNAL OF BIOLOGICAL CHEMISTRY
Vol. 279, No. 20, Issue of May 14, pp. 20889–20897, 2004
Printed in U.S.A.
© 2004 by The American Society for Biochemistry and Molecular Biology, Inc.

Peptidoglycan Induces Nuclear Factor-κB Activation and Cyclooxygenase-2 Expression via Ras, Raf-1, and ERK in RAW 264.7 Macrophages*

Received for publication, October 14, 2003, and in revised form, March 4, 2004
Published, JBC Papers in Press, March 8, 2004, DOI 10.1074/jbc.M311279200

Bing-Chang Chen‡, Ya-Sheng Chang§, Ju-Chiun Kang¶, Ming-Jen Hsu§, Joen-Rong Sheu¶, Ta-Liang Chen‖, Che-Ming Teng, and Chien-Huang Lin‡§‡‡**

*From the ‡School of Respiratory Therapy, §Graduate Institute of Biomedical Technology, the ¶Department of Pharmacology, School of Medicine, Taipei Medical University, the ‖Department of Anesthesiology, Taipei Medical University-Wan Fang Hospital, and **Pharmacological Institute, College of Medicine, National Taiwan University, Taipei 110, Taiwan*

In this study, we investigated the signaling pathway involved in cyclooxygenase-2 (COX-2) expression caused by peptidoglycan (PGN), a cell wall component of the Gram-positive bacterium *Staphylococcus aureus*, in RAW 264.7 macrophages. PGN caused dose- and time-dependent increases in COX-2 expression, which was attenuated by a Ras inhibitor (manumycin A), a Raf-1 inhibitor (GW 5074), and an MEK inhibitor (PD 098059). Treatment of RAW 264.7 macrophages with PGN caused time-dependent activations of Ras, Raf-1, and ERK. The PGN-induced increase in Ras activity was inhibited by manumycin A. Raf-1 phosphorylation at Ser-338 by PGN was inhibited by manumycin A and GW 5074. The PGN-induced increase in ERK activity was inhibited by manumycin A, GW 5074, and PD 098059. Stimulation of cells with PGN activated IκB kinase α/β (IKKα/β), IκBα phosphorylation, IκBα degradation, and κB-luciferase activity. Treatment of macrophages with an NF-κB inhibitor (pyrrolidine dithiocarbamate), an IκBα phosphorylation inhibitor (Bay 117082), and IκB protease inhibitors (L-1-tosylamido-2-phenylethyl chloromethyl ketone and calpain inhibitor I) all inhibited PGN-induced COX-2 expression. The PGN-mediated increase in the activities of IKKα/β and κB-luciferase were also inhibited by the Ras dominant negative mutant (RasN17), manumycin A, GW 5074, and PD 098059. Further studies revealed that PGN induced the recruitment of p85α and Ras to Toll-like receptor 2 in a time-dependent manner. Our data demonstrate for the first time that PGN activates the Ras/Raf-1/ERK pathway, which in turn initiates IKKα/β and NF-κB activation, and ultimately induces COX-2 expression in RAW 264.7 macrophages.

Peptidoglycan (PGN),[1] a cell wall component of Gram-positive bacteria, is an alternating β-linked *N*-acetylmuramyl and *N*-acetylglucosaminyl glycan whose residues are cross-linked by short peptides (1, 2). Like lipopolysaccharide (LPS) as a cell wall component of Gram-negative bacteria, PGN induces most of the clinical manifestations of bacterial infections, including inflammation, fever, septic shock, etc. (3). Most of these effects are due to the activation of macrophages and generation of proinflammatory cytokines, such as tumor necrosis factor α, interleukin (IL)-6, and IL-8 (4–8). PGN binds CD14 and Toll-like receptor 2 (TLR2), which activates transcription factors and induces gene expression (4, 9). Even though it is well known that bacterial products have multiple and various effects on the regulation of host defense and immune responses by macrophages, little is known about how PGN regulates induction of the cyclooxygenase-2 (*cox-2*) gene.

COX is the key enzyme that synthesizes prostaglandins and thromboxane from arachidonic acid (10, 11). Two COX isozymes, COX-1 and COX-2, have been cloned and identified to have 60% homology in humans (12, 13). COX-1, which is constitutively expressed in most tissues, mediates physiological responses and regulates renal and vascular homeostasis. COX-2, an inducible gene for cell synthesis, can be up-regulated by inflammatory stimuli including IL-1β, lipoteichoic acid (LTA), and LPS to produce proinflammatory prostaglandins in inflammation (14–19). Several consensus sequences, including those for nuclear factor-κB (NF-κB), NF-IL6, and the activating transcription factor/cyclic AMP-responsive element in the 5′ region of the *cox-2* gene, have been identified as regulatory sequences that can induce COX-2 in response to various stimuli (20–22). NF-κB, the most important transcription factor for regulating COX-2 expression, is a dimer of the transcription factors p65 or p50 (23). In a resting state, this dimer is associated with IκBs to retain NF-κB in the cytosol (24). IκB kinase (IKK), which is activated through stimulation by cytokines and bacterial products, phosphorylates IκBα at Ser-32 and Ser-36 and IκBβ at Ser-19 and Ser-23 (25–27), to produce ubiquitination of IκBα/β at lysine residues and degradation by the 26 S proteasome (28). This process releases active NF-κB, which is then translocated from the cytosol to the nucleus, to bind specific DNA enhancer sequences and to induce gene transcription (23). A previous report showed that PGN-induced NF-κB acti-

* This work was supported by Grant NSC 92-2314-B-038-059 from the National Science Council of Taiwan. The costs of publication of this article were defrayed in part by the payment of page charges. This article must therefore be hereby marked "*advertisement*" in accordance with 18 U.S.C. Section 1734 solely to indicate this fact.

‡‡ To whom correspondence should be addressed: School of Respiratory Therapy, Taipei Medical University, 250 Wu-Hsing St., Taipei 110, Taiwan. Tel.: 886-2-27361661 (ext. 3510); Fax: 886-2-27397313; E-mail: chlin@tmu.edu.tw.

[1] The abbreviations used are: PGN, peptidoglycan; COX-2, cyclooxygenase-2; DMEM/Ham's F-12, Dulbecco's modified Eagle's medium/Ham's F-12; ERK, extracellular signal-regulated kinase; IKK, IκB kinase; IL, interleukin; IRAK, IL-1 receptor-associated kinase; LPS, lipopolysaccharide; LTA, lipoteichoic acid; MAPK, mitogen-activated protein kinase; MBP, myelin basic protein; MEK, MAPK/ERK kinase; MyD88, myeloid differentiation protein; NF-κB, nuclear factor-κB; PBS, phosphate-buffered saline; PDTC, pyrrolidine dithiocarbamate; Raf-1 RBD, Ras-binding domain for Raf-1; TIR, toll/IL-1 receptor; TLR2, Toll-like receptor 2; TPCK, L-1-tosylamido-2-phenylethyl chloromethyl ketone, TRAF6, tumor necrosis factor receptor-associated factor 6.

vation is mediated through TLR2-dependent multiple signaling molecules including myeloid differentiation protein (MyD88), IL-1 receptor-associated kinase (IRAK), tumor necrosis factor receptor-associated factor 6 (TRAF6), NF-κB-inducing kinase, and the IKK signaling pathway (4, 5), but little information is available about the role of Ras in regulating NF-κB signaling following PGN stimulation.

Ras has been found to couple with multiple effector systems to activate distinct physiological and pathological responses such as cell proliferation and release of proinflammatory mediators (22, 29–31). An important class of Ras effectors is the mitogen-activated protein kinase (MAPK) family. The classic Ras-mediated pathway involves the binding of Raf-1 and subsequent phosphorylation of Raf-1 at Ser-338 by many kinases (32, 33), which in turn activates extracellular signal-regulated kinases (ERKs) (34), and consequently phosphorylates many target proteins including transcription factors and protein kinases (35). Although a role for Ras in COX-2 induction has been implied by many cell types (22, 30, 31), however, PGN-induced COX-2 expression has not been investigated in macrophages. This study was intended to identify the signaling pathway of PGN-induced Ras activation and its roles in PGN-mediated NF-κB activation and COX-2 expression in RAW 264.7 macrophages. Our hypothesis is that PGN might induce TLR2, p85α, and Ras complex formation and subsequently activate the Ras/Raf-1/ERK pathway, which in turn increases IKKα/β activity and NF-κB activation and finally causes COX-2 expression in RAW 264.7 macrophages.

EXPERIMENTAL PROCEDURES

Reagents—Peptidoglycan (PGN derived from *Staphylococcus aureus*) was purchased from Fluka (Buchs, Switzerland). Manumycin A, PD 098059, and SB 203580 were obtained from Calbiochem. GW 5074 was obtained from Tocris (Bristol, UK). Dulbecco's modified Eagle's medium/Ham's F-12 (DMEM/Ham's F-12), fetal calf serum, and penicillin/streptomycin were purchased from Invitrogen. Antibodies specific for α-tubulin and COX-2 were purchased from Transduction Laboratories (Lexington, KY). Protein A/G beads, IκBα protein (amino acids 1–317), antibodies specific for ERK, ERK phosphorylated at Tyr-204, IκBα, IκBα phosphorylated at Ser-32, IKKα, IKKβ, Raf-1, TLR2, Ras, p85α, and anti-mouse and anti-rabbit IgG-conjugated horseradish peroxidase were purchased from Santa Cruz Biotechnology (Santa Cruz, CA). Antibody specific for Raf-1 phosphorylated at Ser-338 was purchased from Cell Signaling and Neuroscience (St. Louis, MO). Anti-mouse and anti-rabbit IgG-conjugated alkaline phosphatases were purchased from Jackson ImmunoResearch (West Grove, PA). pGL2-ELAM-Luc (which is under the control of a single NF-κB-binding site) and pBK-CMV-LacZ were kindly provided by Dr. W.-W. Lin (National Taiwan University, Taipei, Taiwan). A Ras dominant negative mutant (RasN17) and a Ras activity assay kit were purchased from Upstate Biotechnology, Inc. (Lake Placid, NY). [γ-^{32}P]ATP (6,000 Ci/mmol) was purchased from Amersham Biosciences. Bay 117082 was obtained from Alexis (Lausen, Switzerland). GenePORTER™ 2 was purchased from Gene Therapy System (San Diego, CA). All materials for SDS-PAGE were purchased from Bio-Rad. All other chemicals were obtained from Sigma.

Cell Culture—The mouse macrophage cell line, RAW 264.7, was obtained from the American Type Culture Collection (Livingstone, MT), and cells were maintained in DMEM/Ham's F-12 nutrient mixture containing 10% fetal calf serum, 100 units/ml of penicillin G, and 100 μg/ml streptomycin in a humidified 37 °C incubator. After reaching confluence, cells were seeded onto either 6-cm dishes for immunoblotting, co-immunoprecipitation, or kinase assays, or 12-well plates for transfection and κB luciferase assays.

Transfection and κB Luciferase Assays—For these assays, 2×10^5 RAW 264.7 cells were seeded onto 12-well plates, and cells were transfected the following day using GenePORTER™ 2 with 0.5 μg of pGL2-ELAM-Luc and 0.5 μg of pBK-CMV-LacZ. After 24 h, the medium was aspirated, replaced with fresh DMEM/Ham's F12 containing 10% FBS, and then stimulated with PGN (30 μg/ml) for another 24 h before harvest. To assess the effects of Ras, Raf-1, and ERK inhibitors, drugs were added to cells 20 min before PGN addition. To assay the effect of RasN17, cells were co-transfected with RasN17, pGL2-ELAM-Luc, and pBK-CMV-LacZ for 24 h and then treated with PGN. Luciferase activity was determined with a luciferase assay system (Promega) and was normalized on the basis of LacZ expression. The level of induction of luciferase activity was compared as a ratio to cells with and without stimulation.

Immunoblot Analysis—To determine the expressions of COX-2, α-tubulin, ERK phosphorylated at Tyr-204, ERK2, IKKα/β, IκBα phosphorylated at Ser-32, IκBα, Ras, Raf-1 phosphorylated at Ser-338, and Raf-1 in RAW 264.7 macrophages, proteins were extracted, and Western blotting analyses were performed as described previously (36). Briefly, RAW 264.7 macrophages were cultured in 6-cm dishes. After reaching confluence, cells were treated with vehicle and PGN or pretreated with specific inhibitors as indicated followed by PGN. After incubation, cells were washed twice in ice-cold phosphate-buffered saline (PBS) and solubilized in extraction buffer containing 10 mM Tris (pH 7.0), 140 mM NaCl, 2 mM phenylmethylsulfonyl fluoride, 5 mM dithiothreitol, 0.5% Nonidet P-40, 0.05 mM pepstatin A, and 0.2 mM leupeptin. Samples of equal amounts of protein (60 μg) were subjected to SDS-PAGE and then transferred onto a polyvinylidene difluoride membrane that was then incubated in TBST buffer (150 mM NaCl, 20 mM Tris-HCl, and 0.02% Tween 20 (pH 7.4)) containing 5% non-fat milk. Proteins were visualized by specific primary antibodies and then incubated with horseradish peroxidase- or alkaline phosphatase-conjugated second antibodies. Immunoreactivity was detected using enhanced chemiluminescence or nitro blue tetrazolium/5-bromo-4-chloro-3-indolyl phosphate following the manufacturer's instructions. Quantitative data were obtained using a computing densitometer with scientific imaging systems (Eastman Kodak Co.).

Immunoprecipitation and Protein Kinase Assays—RAW 264.7 cells were grown in 6-cm dishes. After reaching confluence, cells were treated with 30 μg/ml PGN for the indicated time intervals or pretreated with specific inhibitors as indicated followed by PGN. After incubation, cells were washed twice with ice-cold PBS, lysed in 1 ml of lysis buffer containing 20 mM Tris-HCl (pH 7.5), 1 mM $MgCl_2$, 125 mM NaCl, 1% Triton X-100, 1 mM phenylmethylsulfonyl fluoride, 10 μg/ml leupeptin, 10 μg/ml aprotinin, 25 mM β-glycerophosphate, 50 mM NaF, and 100 μM sodium orthovanadate, and centrifuged. The supernatant was then immunoprecipitated with respective polyclonal antibodies against IKKα, IKKβ, or ERK2 in the presence of A/G-agarose beads overnight. The beads were washed three times with lysis buffer and two times with kinase buffer containing 20 mM HEPES (pH 7.4), 20 mM $MgCl_2$, and 2 mM dithiothreitol. The kinase reactions were performed by incubating immunoprecipitated beads with 20 μl of kinase buffer supplemented with 20 μM ATP and 3 μCi of [γ-^{32}P]ATP at 30 °C for 30 min. To assess IKKα/β and ERK activities, 0.5 μg of GST-IκBα protein (amino acids 1–317) and 50 μg/ml of myelin basic protein (MBP) were respectively added as the substrates. The reaction mixtures were analyzed by 12 (IKKα/β) or 15% (ERK) SDS-PAGE followed by autoradiography.

Ras Activity Assay—Ras activity was measured using a Ras activity assay kit. The assay was performed according to the manufacturer's instructions. Briefly, cells were washed twice with ice-cold PBS, lysed in magnesium lysis buffer (MLB) (25 mM HEPES (pH 7.5), 150 mM NaCl, 5% Igepal CA-630, 10 mM $MgCl_2$, 5 mM EDTA, 10% glycerol, 10 μg/ml aprotinin, and 10 μg/ml leupeptin), and centrifuged. An equal volume of lysate was incubated with 5 μg of Ras-binding domain for Raf-1 (Raf-1 RBD) at 4 °C overnight, and the beads were washed three times with MLB lysis buffer. Bound Ras proteins were then solubilized in 2× Laemmli sample buffer and quantitatively detected by Western blotting (10% SDS-PAGE) using mouse monoclonal Ras with the ECL system and by densitometry of corresponding bands using scientific imaging systems.

Co-immunoprecipitation of TLR2 Complex Formation—RAW 264.7 cells were grown in 6-cm dishes. After reaching confluence, cells were treated with 30 μg/ml PGN for the indicated time intervals. The cells were harvested, lysed in 1 ml of PD buffer (40 mM Tris-HCl (pH 8.0), 500 mM NaCl, 0.1% Nonidet P-40, 6 mM EGTA, 10 mM β-glycerophosphate, 10 mM NaF, 300 μM sodium orthovanadate, 2 mM phenylmethylsulfonyl fluoride, 10 μg/ml aprotinin, 1 μg/ml leupeptin, and 1 mM dithiothreitol), and centrifuged. The supernatant was then immunoprecipitated with specific antibodies against TLR2, p85α, or Ras in the presence of protein A/G beads at 4 °C overnight. The immunoprecipitated beads were washed three times with PD buffer. The samples were fractionated on 15 (for Ras) or 8% (for TLR2 or p85α) SDS-PAGE, transferred to a polyvinylidene difluoride membrane, and subjected to immunoblot analysis with antibodies specific for Ras, TLR2, or p85α.

Statistical Analysis—Results are presented as the mean ± S.E. from at least three independent experiments. One-way analysis of variance followed by, when appropriate, Bonferroni's multiple range test was used to determine the statistical significance of the difference between

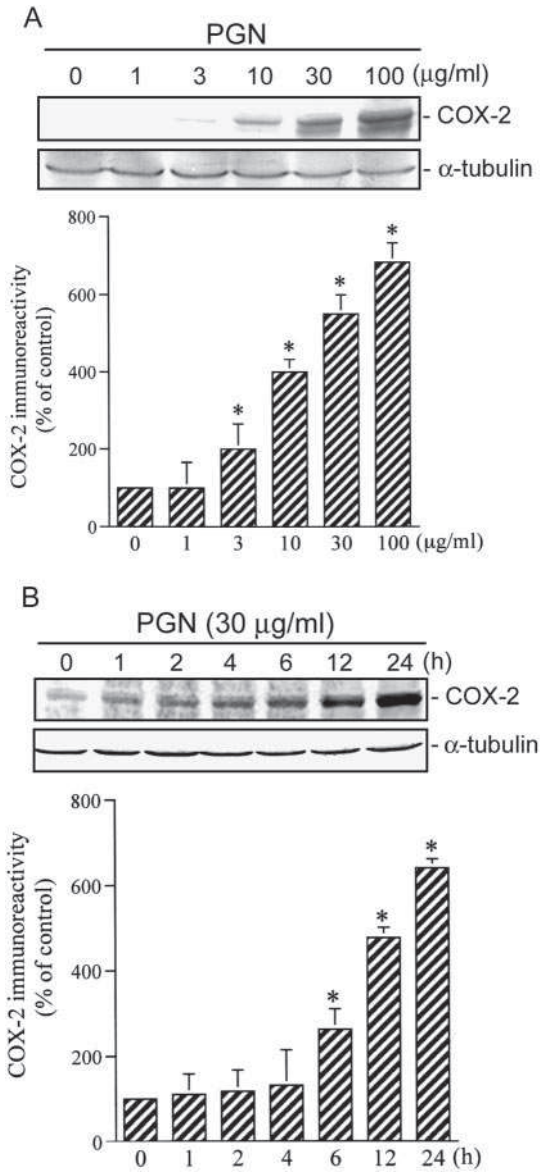

FIG. 1. **Concentration- and time-dependent increases in COX-2 expression by PGN in RAW 264.7 macrophages.** *A*, macrophages were incubated with various concentrations of PGN for 24 h, and then COX-2 or α-tubulin protein levels were determined. *B*, cells were incubated with 30 μg/ml PGN for the indicated time intervals, and then COX-2 or α-tubulin protein levels were determined. Equal loading in each lane is shown by the similar intensities of α-tubulin. Traces represent results from three independent experiments, which are presented as the mean ± S.E. *, $p < 0.05$ as compared with the control group.

means. A p value of less than 0.05 was considered statistically significant.

RESULTS

PGN Induces Macrophage COX-2 Expression—Murine RAW 264.7 macrophages were chosen to investigate the signal pathways of PGN in COX-2 expression, an inflammatory response gene. Treatment with PGN (1–100 μg/ml) for 24 h induced COX-2 protein expression in a concentration-dependent manner (Fig. 1*A*); this induction also occurred in a time-dependent manner (Fig. 1*B*). After 24 h of treatment with 30 μg/ml PGN, the COX-2 protein had increased by ~640 ± 14% ($n = 3$) (Fig. 1*B*). To further confirm this stimulation-specific mediation by PGN without LPS contamination, polymycin B, an LPS inhibitor, was tested. We found that polymycin B (0.3 μg/ml) did not change PGN-induced COX-2 protein levels. In contrast, polymycin B completely inhibited LPS (1 μg/ml)-induced COX-2 protein expression (data not shown).

Augmentation of COX-2 Expression Occurred at the Level of Transcription—RAW 264.7 macrophages were pretreated with either actinomycin D (a transcriptional inhibitor) or cycloheximide (a translational inhibitor) and then treated with 30 μg/ml PGN. As a result, the PGN-induced elevation of COX-2 expression was inhibited by actinomycin D (30 nM) and cycloheximide (100 nM) by about 55 ± 4 and 72 ± 6%, respectively ($n = 3$) (Fig. 2*A*). The results suggest that the increase in COX-2 protein in RAW 264.7 macrophages responsive to PGN may have been due to COX-2 transcriptional expression.

Involvement of NF-κB in PGN-induced COX-2 Expression—As mentioned previously, NF-κB activation is necessary for COX-2 induction. Pyrrolidine dithiocarbamate (PDTC), an antioxidant, has been shown to inactivate NF-κB in macrophages (37). To examine whether NF-κB activation is involved in the signal transduction pathway leading to COX-2 expression caused by PGN, the NF-κB inhibitor PDTC was used. Fig. 2*B* shows that PGN-induced COX-2 protein levels were inhibited by PDTC (5–50 μM) in a concentration-dependent manner. When cells were treated with 50 μM PDTC, PGN-induced COX-2 expression was inhibited by 64 ± 4% ($n = 3$). Furthermore, macrophage pretreatment with an IκBα phosphorylation inhibitor (Bay 117082) (38) inhibited PGN-induced COX-2 protein expression in a concentration-dependent manner. Pretreatment of cells with 10 μM Bay 117082 inhibited the PGN response by 53 ± 3% ($n = 3$) (Fig. 2*C*). In parallel with the inhibition by PDTC and Bay 117082, IκB protease inhibitors (L-1-tosylamido-2-phenylenylethyl chloromethyl ketone (TPCK, 3 μM) and calpain inhibitor I (10 μM)) (39, 40) also inhibited PGN-induced COX-2 protein expression by 35 ± 3 and 65 ± 5%, respectively ($n = 3$) (Fig. 2*D*). These results suggest that NF-κB activation is necessary for PGN-induced COX-2 expression in RAW 264.7 macrophages.

PGN Causes Increases in IKKα/β Activity, IκBα Phosphorylation, IκBα Degradation, and κB-Luciferase Activity—We further determined the upstream molecules of NF-κB in PGN-induced NF-κB activation. Stimulation of cells with 30 μg/ml PGN induced increases in IKKα/β activity and IκBα phosphorylation in a time-dependent manner, reaching maximums after 10 and 10–30 min of treatment, respectively (Fig. 3, *A* and *B*). In parallel with IKKα/β activity and IκBα phosphorylation, IκBα degradation was apparent after 10 min of treatment with 30 μg/ml PGN, and the IκBα protein was resynthesized after 60 min of treatment (Fig. 3*C*). To directly determine NF-κB activation after PGN treatment, RAW 264.7 macrophages were transiently transfected with pGL2-ELAM-κB-luciferase as an indicator of NF-κB activation. As shown in Fig. 3*D*, macrophage treatment with PGN (1–100 μg/ml) for 24 h caused a concentration-dependent increase in κB luciferase activity.

Ras Is Involved in PGN-induced COX-2 Expression—To explore whether Ras might mediate PGN-induced COX-2 expression, manumycin A, a Ras inhibitor (41), was used. As shown in Fig. 4*A*, pretreatment of RAW 264.7 macrophages with manumycin A inhibited PGN-induced COX-2 expression in a concentration-dependent manner. When cells were treated with 3 μM manumycin A, PGN-induced COX-2 expression was inhibited by 58 ± 2% ($n = 3$). However, manumycin A had no effect on the basal level of COX-2 expression (Fig. 4*A*). Moreover, we found that 3 μM manumycin A also inhibited 1 μg/ml LPS-stimulated COX-2 expression by 72 ± 8% ($n = 3$) (Fig. 4*A*). Next, we directly measured the Ras activity in response to PGN and LPS. Fig. 4, *B* and *C*, shows that treatment of RAW 264.7 cells with 30 μg/ml PGN or 1 μg/ml LPS induced an increase in Ras activity in a time-de-

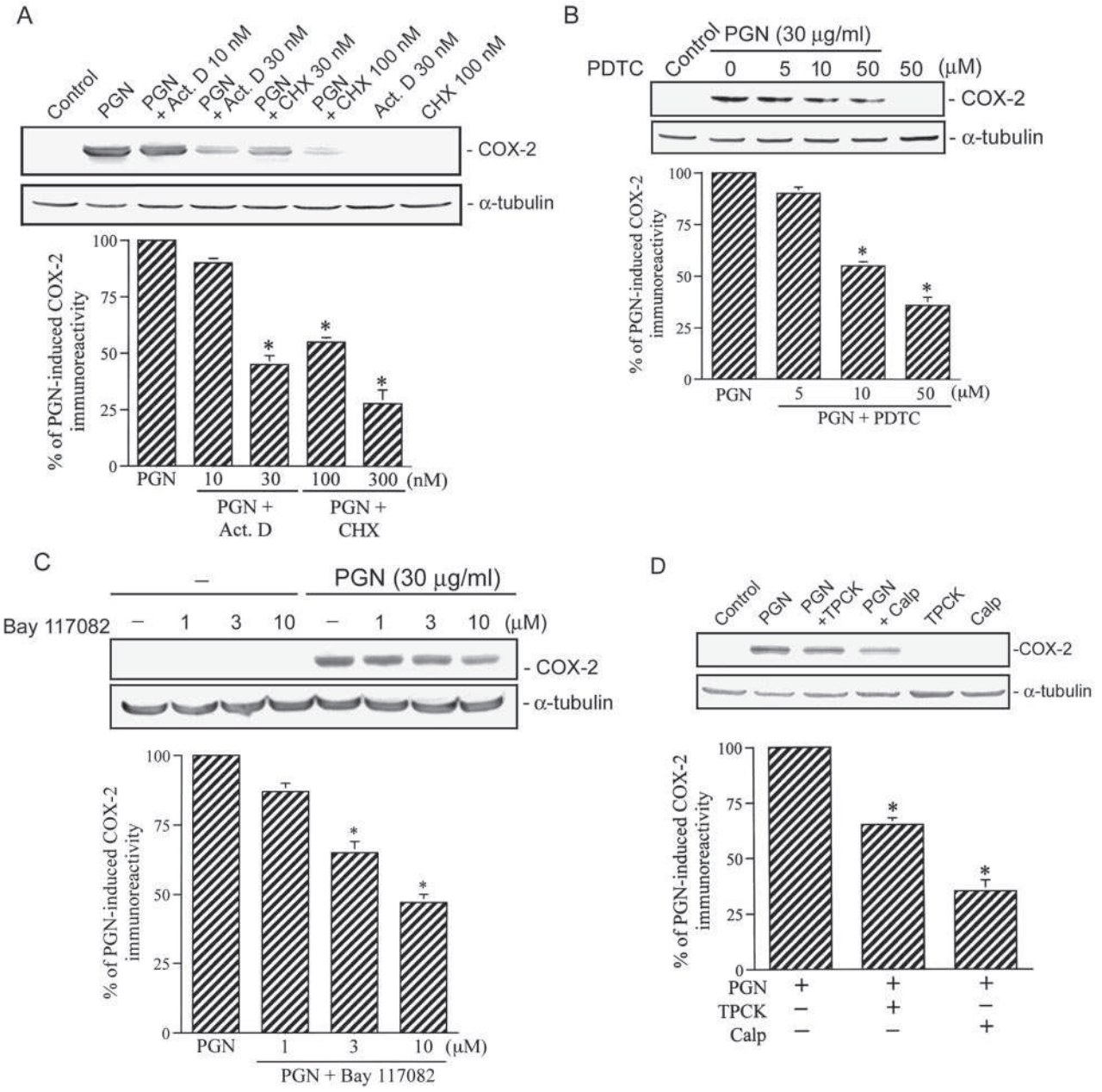

FIG. 2. **NF-κB is involved in PGN-mediated COX-2 induction in RAW 264.7 macrophages.** *A*, transcriptional activity is involved in PGN-induced COX-2 expression. Cells were pretreated for 30 min with vehicle, 10–30 nM actinomycin D (*Act. D*), and 30–100 nM cycloheximide (*CHX*) and then stimulated with 30 μg/ml PGN for 24 h. Cells were lysed and then immunoblotted for COX-2 or α-tubulin. *B–D*, the NF-κB signal pathway was necessary for PGN-induced COX-2 expression. Cells were pretreated for 30 min with 5–50 μM PDTC (*B*), 1–10 μM Bay 117082 (*C*), or 3 μM TPCK and 10 μM calpain inhibitor I (*Calp*) (*D*) and then stimulated with 30 μg/ml PGN for 24 h. Cell were lysed and then immunoblotted for COX-2 or α-tubulin. Equal loading in each lane is demonstrated by the similar intensities of α-tubulin. Results are representative of three independent experiments. Traces represent results from three independent experiments, which are presented as the mean ± S.E. *, $p < 0.05$ as compared with PGN treatment.

pendent manner, as assessed by immunoblotting samples for Ras immunoprecipitated from lysates using Raf-1-RBD. Maximal activation was detected after 5 min of stimulation, and the response continued until 30 min after PGN stimulation (Fig. 4*B*). Similarly, the LPS-induced increase in Ras activity began at 3 min, peaked at 5 min, and then declined at 10 min after LPS treatment (Fig. 4*C*). Furthermore, the PGN-induced increase in Ras activity was markedly inhibited by pretreatment of cells for 30 min with manumycin A (1–3 μM) in a concentration-dependent manner (Fig. 4*D*). Taken together, these results imply that Ras activation is involved in PGN- or LPS-induced COX-2 expression.

Raf-1 Is Involved in PGN-induced COX-2 Expression—To examine whether Raf-1, a target protein for Ras, might play a crucial role in PGN-induced COX-2 expression, the Raf-1 inhibitor GW 5074 (42) was used. As shown in Fig. 5*A*, 1 μM of GW 5074 alone did not affect the basal COX-2 level, but it significantly inhibited PGN-induced COX-2 expression by 43 ± 3% ($n = 3$). Furthermore, we found that GW 5074 (1 μM) inhibited LPS-induced COX-2 expression by 76 ± 3% ($n = 3$) (Fig. 5*A*). Raf-1 is associated with Ras-GTP and then by additional modifications such as phosphorylation at Ser-338 to become the active form (33). The activated Raf-1 then triggers sequential activation of downstream molecules. Thus, phosphorylation of Raf-1 at Ser-338 is a critical step in Raf-1 activation. Next, we further examined Raf-1 Ser-338 phosphorylation by

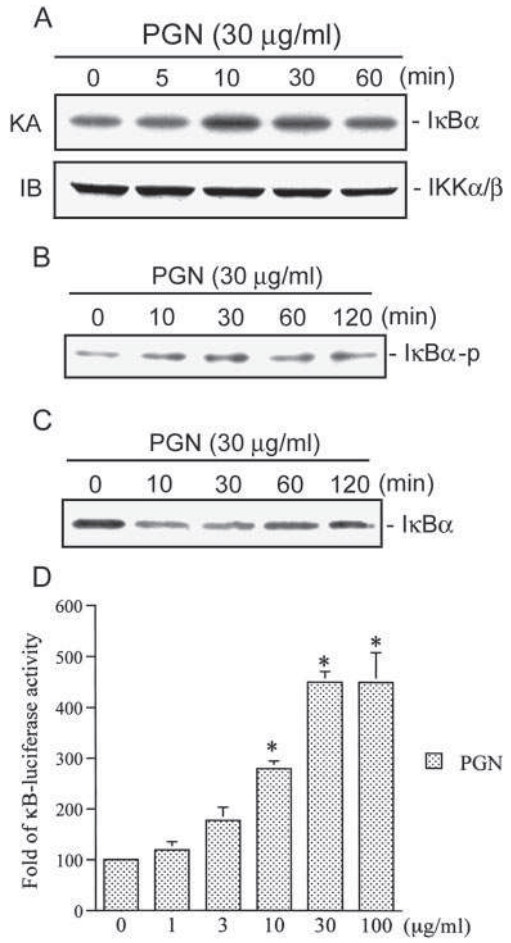

FIG. 3. **PGN induced IKKα/β activation, IκBα phosphorylation, IκBα degradation, and κB-luciferase activity in RAW 264.7 macrophages.** *A*, RAW 264.7 cells were incubated with 30 μg/ml PGN for 0–60 min, and cell lysates were then immunoprecipitated with antibodies specific for IKKα and IKKβ. One set of immunoprecipitates was subjected to the kinase assay (*KA*) described under "Experimental Procedures" using the GST-IκBα fusion protein as a substrate (*top panel*). The other set of immunoprecipitates was subjected to 10% SDS-PAGE and analyzed by immunoblotting (*IB*) with the anti-IKKα/β antibody (*bottom panel*). Equal amounts of the immunoprecipitated kinase complex present in each kinase assay were confirmed by immunoblotting for IKKα/β. *B* and *C*, following incubation for 0–120 min with 30 μg/ml PGN, IκBα phosphorylation (*B*) and IκBα degradation (*C*) were determined by immunoblotting using phospho-IκBα- and IκBα-specific antibodies, respectively. Typical traces are representative of three experiments with similar results. *D*, RAW 264.7 macrophages were transiently transfected with 0.5 μg of pGL2-ELAM-Luc and 0.5 μg of pBK-CMV-LacZ for 24 h, and then cells were incubated with 1–100 μg/ml PGN for another 24 h. Luciferase activities were determined as described under "Experimental Procedures." The level of induction of luciferase activity was compared with that of cells without PGN treatment. Data represent the mean ± S.E. of three to four experiments performed in duplicate. *, $p < 0.05$ as compared with the control without PGN treatment.

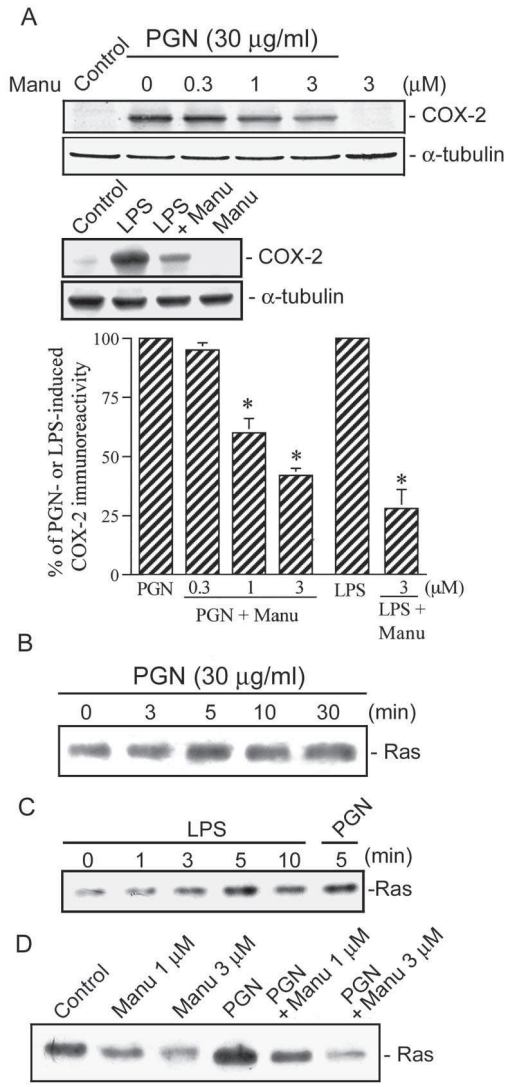

FIG. 4. **Effects of manumycin A on PGN-induced COX-2 expression and Ras activation in RAW 264.7 macrophages.** *A*, RAW 264.7 macrophages were pretreated with vehicle and 0.3–3 μM manumycin A (*Manu*) for 30 min followed by stimulation with 30 μg/ml PGN or 1 μg/ml LPS for another 24 h, and COX-2 expression was determined by immunoblotting with an antibody specific for COX-2. Equal loading in each lane is demonstrated by the similar intensities of α-tubulin. Typical traces are representative of three experiments with similar results, which are presented as the mean ± S.E. *, $p < 0.05$ as compared with PGN or LPS treatment. *B* and *C*, RAW 264.7 macrophages were incubated with 30 μg/ml PGN or 1 μg/ml LPS for indicated time intervals, and cell lysates were then immunoprecipitated with an antibody specific for Raf-1 RBD. The Ras activity assay is described under "Experimental Procedures." Typical traces represent three experiments with similar results. *D*, cells were pretreated with 1–3 μM manumycin A (*Manu*) for 30 min and then treated with 30 μg/ml PGN for another 10 min. Cells were then lysed for Ras activity assay as described above. Typical traces represent two experiments with similar results.

PGN stimulation in RAW 264.7 macrophages using the anti-phospho-Raf-1 antibody at Ser-338. When cells were treated with 30 μg/ml PGN for various time intervals, Raf-1 Ser-338 phosphorylation increased at 5 min and peaked at 10 min. After 20 min of treatment, the PGN-induced increase in Raf-1 Ser-338 phosphorylation declined (Fig. 5*B*). In addition, PGN-induced Raf-1 Ser-338 phosphorylation was also inhibited by treatment with 3 μM manumycin A and 1 μM GW 5074 (Fig. 5*C*). Results indicate that Raf-1 is a downstream molecule of Ras and is involved in Ras-mediated COX-2 protein expression.

PGN Mediates Phosphorylation of ERK—We next wished to determine whether PGN is able to activate ERK, a critical downstream target of Raf-1 (43), which has been shown to induce gene expression (44). We tested the role of ERK in mediating PGN-induced COX-2 expression by using the specific MEK inhibitor PD 098059. As shown in Fig. 6*A*, PGN-induced COX-2 expression was markedly attenuated by pretreatment of cells with PD 098059 (3–30 μM) in a concentration-dependent manner. Pretreatment of cells with 30 μM PD 098059 inhibited PGN-induced COX-2 expression by 85 ± 7% ($n = 3$) (Fig. 6*A*). Moreover, we also found that 30 μM PD 098059 inhibited LPS-induced COX-2 expression by 76 ± 5% ($n = 3$) (Fig. 6*A*). To directly confirm the crucial role of ERK in COX-2 expression, we determined ERK phosphorylation and kinase activity in response to PGN. As

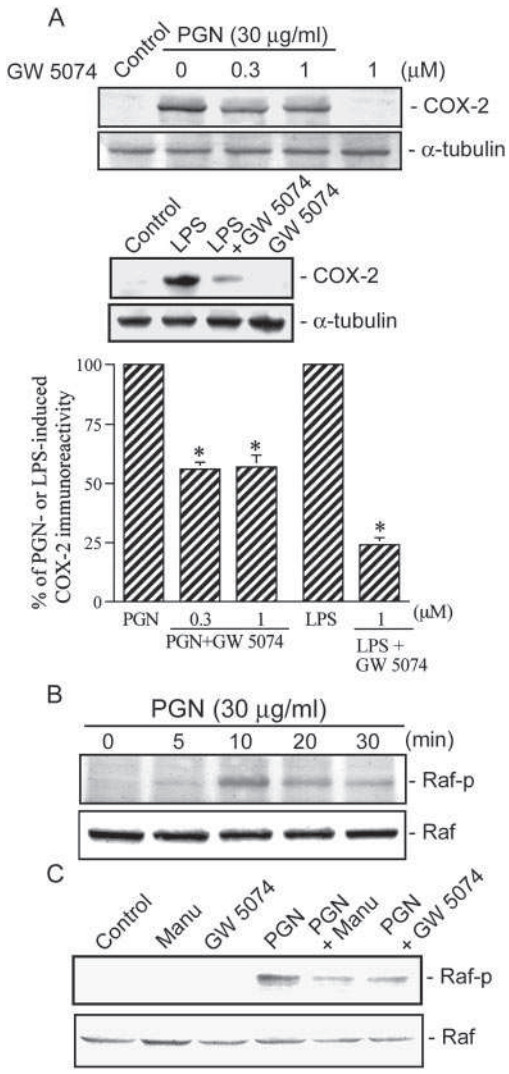

FIG. 5. **Effects of GW 5074 on PGN-induced COX-2 expression and Raf-1 phosphorylation in RAW 264.7 macrophages.** *A*, RAW 264.7 macrophages were pretreated with vehicle and GW 5074 (0.3–1 μM) for 30 min followed by stimulation with 30 μg/ml PGN or 1 μg/ml LPS for another 24 h, and COX-2 expression was determined by immunoblotting with an antibody specific for COX-2. Equal loading in each lane is demonstrated by the similar intensities of α-tubulin. Typical traces represent three experiments with similar results, which are presented as the mean ± S.E. *, $p < 0.05$ as compared with PGN or LPS treatment. *B*, RAW 264.7 macrophages were incubated with 30 μg/ml PGN for 0–30 min, and then Raf-1 phosphorylation (*upper panel*) and Raf-1 (*bottom panel*) protein levels were determined. The presence of equal loading in each lane is shown by the similar intensities of Raf-1. Traces represent results from three independent experiments. *C*, cells were pretreated with 3 μM manumycin A (*Manu*) or 0.3 μM GW 5074 for 30 min, and then treated with 30 μg/ml PGN for another 10 min. Cells were then lysed for Raf-1 phosphorylation (*upper panel*) and Raf-1 (*bottom panel*) protein levels as described above. Typical traces represent two experiments with similar results.

shown in Fig. 6*B*, treatment of RAW 264.7 macrophages with 30 μg/ml PGN resulted in a time-dependent phosphorylation of ERK. The ERK phosphorylation began at 10 min, peaked at 30–60 min, and then declined to 120 min after PGN treatment (Fig. 6*B*, *upper panel*). The protein level of ERK2 was not affected by PGN treatment (Fig. 6*B, bottom panel*). In parallel, using MBP as an ERK substrate, an increase in ERK activity was observed within 10 min and reached a peak 30 min after PGN stimulation, thereafter declining to 60 min after stimulation (Fig. 6*C*). To determine the relationships among Ras, Raf-1, and ERK in the PGN-mediated signaling pathway, we found that pretreatment of RAW 264.7 cells for 30 min with 3 μM manumycin A, 1 μM GW 5074, and 30 μM PD 098059 markedly inhibited the PGN-induced increase in ERK activity (Fig. 6*D*). Based on these results, we suggest that activation of Ras and Raf-1 occurs upstream of ERK in the PGN-induced signaling pathway.

Ras, Raf-1, and ERK Mediated PGN-induced IKKα/β and NF-κB Activation—We further examined whether the activation of IKKα/β and NF-κB occurs through the Ras/Raf-1/ERK signaling pathway. As shown in Fig. 7*A*, pretreatment of cells for 30 min with manumycin A (3 μM), GW 5074 (1 μM), and PD 098059 (30 μM) markedly attenuated the PGN-induced increase in IKKα/β activity. None of these inhibitors affected the basal IKKα/β activity (Fig. 7*A*). Similarly, the PGN-induced increase in κB-luciferase activity was also inhibited by 3 μM manumycin A, 1 μM GW 5074, and 30 μM PD 098059 by 74 ± 11, 71 ± 6, and 58 ± 13%, respectively ($n = 3$) (Fig. 7*B*). To confirm further the role of Ras in PGN-mediated NF-κB activation, RasN17 was tested. Transfection of RAW 264.7 cells with RasN17 inhibited the PGN-induced increase in κB-luciferase activity in a dose-dependent manner, with 1 μg of RasN17 reducing the basal κB-luciferase activity and PGN response by about 64 ± 15 and 82 ± 7%, respectively ($n = 3$) (Fig. 7*B*). Taken together, these data suggest that activation of Ras/Raf-1/ERK pathway is also required for PGN-induced IKKα/β and NF-κB activation in RAW 264.7 macrophages.

Ras Is Associated with TLR2 by p85α upon PGN Stimulation—The rapid activation of Ras by PGN stimulation suggested that Ras activation might occur close to TLR2 in the PGN signal pathway. Therefore, we investigated whether PGN can induce the interaction between Ras and TLR2. As shown in Fig. 8*A*, treatment of RAW 264.7 macrophages with 30 μg/ml PGN led to the rapid association of Ras and TLR2, as detected by immunoblotting using the antibody to Ras after immunoprecipitation of TLR2. The association of TLR2 and Ras occurred at 1 min and peaked at 3–5 min (Fig. 8*A*). Control experiments using an unrelated polyclonal antibody for immunoprecipitation showed no Ras binding (Fig. 8*A*). The interaction between TLR2 and Ras was further confirmed by converse experiments in which the TLR2 and Ras complex was immunoprecipitated with the Ras antibody and immunoblotted with the TLR2 antibody (Fig. 8*B*). Previous reports (45) showed that p85 can interact with TLR2 and then induces Rac activation. Therefore, we further examined the role of p85α involvement in TLR2 and Ras complex formation by PGN stimulation. Fig. 8*C* shows that PGN (30 μg/ml) treatment rapidly increased the formation of the TLR2 and p85α complex at as early as 30 s and then it declined at 1–5 min. We also found that treatment of macrophages with PGN induced the association of p85α and Ras within 1 min, and this was sustained for 5 min (Fig. 8*D*). These results suggested that PGN induces Ras activation by interacting with TLR2 and p85α in macrophages.

DISCUSSION

The findings of this study showed that PGN induces COX-2 expression through activation of the Ras/Raf-1/ERK/IKKα/β/NF-κB signal pathway in RAW 264.7 macrophages. In mice and humans, the COX-2 promoter has many transcription factors including NF-κB in the 5′ region of the *cox-2* gene (20–22). Transcription factor NF-κB has been reported to induce macrophage COX-2 in response to various inflammatory stimuli (46). Previous studies have demonstrated that NF-κB activation is necessary for LPS-induced COX-2 induction in RAW 264.7 macrophages (47–50). Hwang *et al.* (47, 48) reported that in LPS-treated RAW 264.7 macrophages, NF-κB plays a crucial role in TLR4-induced *cox-2* gene expression. The results of this study showed that NF-κB activation also contributed to PGN-induced COX-2 induction in RAW 264.7 macrophages (Fig. 2, and that all inhibitors of the NF-κB-dependent signaling path-

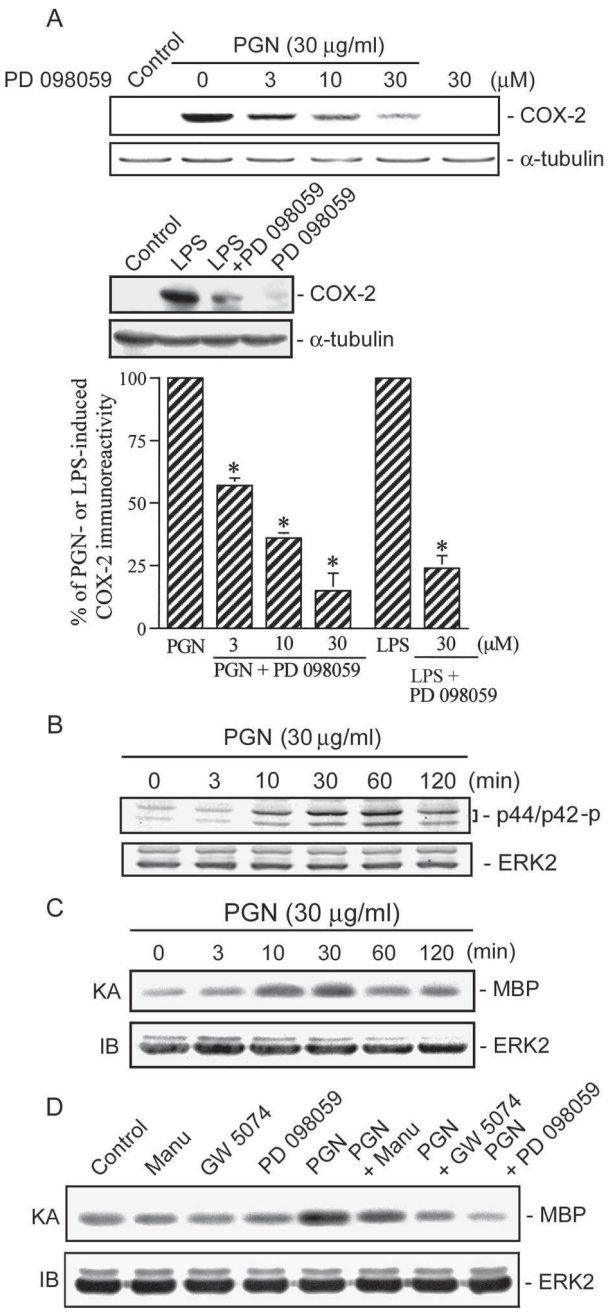

FIG. 6. **Effects of PD 098059 on PGN-induced COX-2 expression, ERK phosphorylation, and ERK activity in RAW 264.7 macrophages.** *A*, RAW 264.7 macrophages were pretreated with vehicle and PD 098059 (3–30 μM) for 30 min before treatment with 30 μg/ml PGN or 1 μg/ml LPS for another 24 h, and COX-2 expression was determined by immunoblotting with an antibody specific for COX-2. Equal loading in each lane is shown by the similar intensities of α-tubulin. Typical traces represent three experiments with similar results, which are presented as the mean ± S.E. *, $p < 0.05$ as compared with PGN or LPS treatment. *B*, after cells were treated with 30 μg/ml PGN for different intervals, ERK phosphorylation was shown by immunoblotting with an antibody specific for phosphorylated ERK (*upper panel*). Equal loading in each lane is shown by the similar intensities of ERK2 (*bottom panel*). Typical traces represent three experiments with similar results. *C*, for ERK kinase activity, cell lysates were immunoprecipitated with ERK2 antibody. One set of immunoprecipitates was subjected to the kinase assay (*KA*) using MBP as a substrate. The other set of immunoprecipitates was subjected to 12% SDS-PAGE and analyzed by immunoblotting (*IB*) with an anti-ERK2 antibody. Equal amounts of the immunoprecipitated kinase complexes present in each kinase assay were confirmed by immunoblotting for ERK2. Shown are representative results from three independent experiments. *D*, cells were pretreated with 3 μM manumycin A (*Manu*), 0.3 μM GW 5074, and 30 μM PD 098059 for 20 min and then incubated with 30 μg/ml PGN for another 10 min. Cell lysates were immunoprecipitated with an antibody specific for ERK2. The kinase assay (*KA*) and immunoblotting (*IB*) were as described above. Equal amounts of the immunoprecipitated kinase complexes present in each kinase assay were confirmed by immunoblotting for ERK2. The data shown represent three experiments.

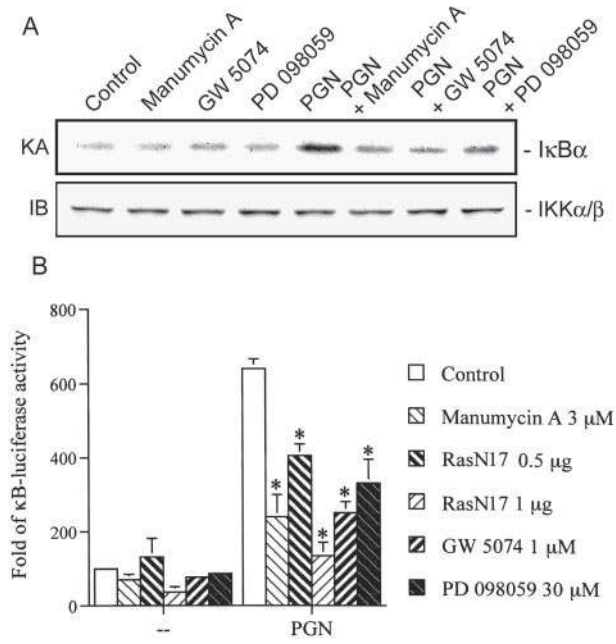

FIG. 7. **The Ras/Raf-1/ERK signal pathway is involved in PGN-mediated IKKα/β and NF-κB activation in RAW 264.7 macrophages.** *A*, RAW 264.7 macrophages were pretreated with vehicle, 3 μM manumycin A (*Manu*), 0.3 μM GW 5074, and 30 μM PD 098059 for 30 min followed by stimulation with 30 μg/ml PGN for another 20 min; cell lysates were then immunoprecipitated with antibodies specific to IKKα and IKKβ. One set of immunoprecipitates was subjected to the kinase assay (*KA*) by using the GST-IκBα fusion protein as a substrate (*top panel*). The other set of immunoprecipitates was subjected to 10% SDS-PAGE and analyzed by immunoblotting (*IB*) with anti-IKKα/β antibody (*bottom panel*). Equal amounts of the immunoprecipitated kinase complex present in each kinase assay were confirmed by immunoblotting for IKKα/β. *B*, RAW 264.7 macrophages were either transiently transfected with 0.5 μg of pGL2-ELAM-Luc and 1 μg of pBK-CMV-LacZ for 24 h and were co-transfected with 0.5 and 0.5 μg of RasN17, or were pretreated with 3 μM manumycin A, 0.3 μM GW 5074, and 30 μM PD 098059 for 20 min and then stimulated with 30 μg/ml PGN for another 24 h. Cells were harvested for luciferase assay as described in Fig. 4*C*. Data represent the mean ± S.E. of three experiments performed in duplicate. *, $p < 0.05$ as compared with the corresponding control response of PGN treatment.

way, including PDTC, Bay 117082, TPCK, and calpain inhibitor I, inhibited PGN-induced macrophage COX-2 expression. Furthermore, PGN induced IKKα/β activation, IκBα phosphorylation, and IκBα degradation, as well as an increase in κB-luciferase activity. These findings are in agreement with those from studies on LTA (16, 51), another cell wall component of Gram-positive bacteria. NF-κB activation is required to induce COX-2 transcription in epithelial cells. The results of this study also showed that Ras, Raf-1, and ERK are involved in NF-κB activation through an increase in IKKα/β activity. A previous report showed that in transformed liver epithelial cells, Ras and Raf-1 lead to constitutive activation of NF-κB through the IKKα/β complex (52). These pathways may mediate PGN effect. As shown in Fig. 7, manumycin A, GW 5074, and PD 098059 blocked PGN-induced IKKα/β activity. In addition, RasN17 and these inhibitors attenuated induction of NF-κB reporter activity or *cox-2* gene expression, implying a role in the pathway of transactivation by PGN stimulation.

The TLR family now consists of 10 different TLRs (TLR1-TLR10), but only TLR2 and TLR4 are known to have biological

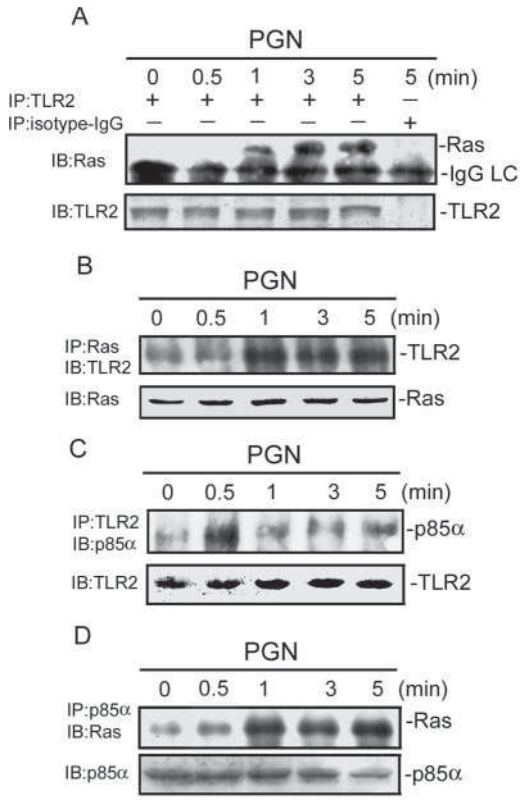

FIG. 8. **Ras is associated with p85α and TLR2 upon PGN stimulation in RAW 264.7 macrophages.** *A*, RAW 264.7 macrophages were stimulated with 30 μg/ml PGN for 0–5 min and were then lysed. Cells extracts were immunoprecipitated (*IP*) with anti-TLR2 or anti-isotype IgG antibody and then immunoblotted (*IB*) with anti-Ras antibody. IgG LC (IgG light chain). *B*, RAW 264.7 macrophages were treated with PGN for the indicated time intervals. Cells extracts were immunoprecipitated with the anti-Ras antibody and then immunoblotted with the anti-TLR2 antibody. *C*, cells were treated with PGN for 0–5 min, then immunoprecipitated with the anti-TLR2 antibody, and immunoblotted with the anti-p85α antibody. *D*, cells were stimulated with PGN for 0–5 min, then immunoprecipitated with the anti-p85 α antibody, and immunoblotted with the anti-Ras antibody. Typical traces are representative of three experiments with similar results.

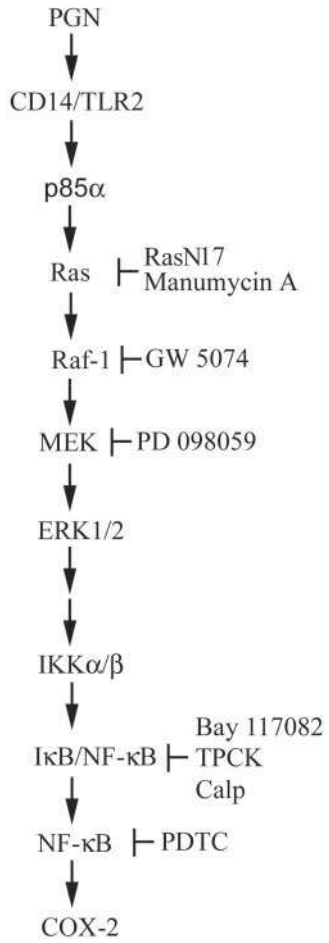

FIG. 9. **Schematic summary of signal transduction by PGN induces COX-2 expression in RAW 264.7 macrophages.** PGN-induced Ras activation may occur through the recruitment of p85α and Ras to TLR2 in RAW 264.7 macrophages. The PGN-induced activation of the Ras/Raf-1/ERK cascade results in an increase in IKKα/β activity, IκBα degradation, and NF-κB activation, which leads to expression of the macrophage COX-2.

and pathological functions (53, 54). The cytoplasmic portion of TLRs shows high similarity to that of the IL-1 receptor family and is now called the Toll/IL-1 receptor (TIR) domain (53). Upon recognizing respective ligands, the TIR domain recruits MyD88/IRAK/TRAF6 and activates downstream signaling molecules such as MAPK and NF-κB (53). In addition to the common MyD88/IRAK/TRAF6 pathway, the TIR domain family can activate downstream signal components through small G proteins such as Rac and Ras to mediate NF-κB activation and COX-2 expression (55, 56). To date, how the TIR domain family activates Ras, especially TLR2, is still not clear. Recently, Ras activation has been shown to be involved in the signaling pathway of IL-1-induced p38 MAPK activation and occurred through associating with IRAK, IRAK2, TRAF6, and TAK1 multiprotein complex in EL4.NOB-1 cells and HeLa cells (57, 58). Furthermore, Ras was found to participate in CpG oligonucleotide-induced COX-2 expression through association with TLR9 and to activate ERK and NF-κB in RAW 264.7 macrophages (56). In addition, a previous study also showed that the TIR domain of TLR2 contains a p85-binding motif (Y*XX*M), which contributes to Rac mediation of TLR2-induced NF-κB activation via the recruitment of p85 and Rac to the TLR2 (45). The findings of our experiments showed that PGN can rapidly induce TLR2 association with p85α as early as 30 s, and subsequently Ras interacted with TLR2 at 1 min following PGN treatment. Simultaneously, we also found that PGN induced the association of Ras and p85α during the interaction of Ras and TLR2. Based on these findings, we suggest that PGN-induced Ras activation may occur through the recruitment of p85α and Ras to TLR2 in RAW 264.7 macrophages.

Ras, an oncogenic protein, plays a critical role in the induction of COX-2 protein (59, 60). Ras might activate a number of signal pathways, including the Raf-1/MEK/ERK pathway and the phosphatidylinositol 3-kinase/Akt/NF-κB pathway (34, 59, 60). In RAW 264.7 macrophages, LPS induces tumor necrosis factor gene expression through the Ras/Raf-1/MEK/ERK pathway (61). In murine fibroblasts, oncogene- and growth factor-induced COX-2 transcription requires Ras-dependent Raf-2/MAPKK/ERK activation (60). In this study, we found that treatment of RAW 264.7 macrophages with PGN caused sequential activations of Ras, Raf-1, and ERK, and that manumycin A, GW 5074, and PD 098059 all inhibited PGN-induced ERK activation and COX-2 expression. These results suggested that the Ras/Raf-1/ERK signal pathway is important for PGN-induced COX-2 expression. This suggestion is further supported by our previous report that LTA induces COX-2 expression through the ERK pathway to induce NF-κB activation in human lung epithelial cells (62). However, the contribution of Ras or ERK to LPS-mediated RAW 264.7 macrophages COX-2 expression is controversial. Most reports (47, 50, 63–65) have shown that LPS-induced RAW 264.7 macrophages *cox-2* gene

expression is dependent on the ERK signaling pathway. However, Wadleigh *et al.* (66) showed that overexpression of a dominant negative mutant of Ras or ERK did not inhibit LPS-induced COX-2 luciferase reporter activity. Nevertheless, they did not directly measure Ras or ERK activity. In the present study, we found that LPS induced an increase in Ras activity and that manumycin A, GW 5074, and PD 098059 all attenuated LPS-mediated COX-2 expression. Taken together, our results indicate that the Ras/Raf-1/ERK signaling pathway is also necessary for LPS-induced COX-2 expression in RAW 264.7 macrophages.

In conclusion, the findings of our study for the first time showed that PGN induced COX-2 transcription through the Ras/Raf-1/ERK signaling pathway to increase in IKKα/β activity, NF-κB activation, and COX-2 expression in RAW 264.7 macrophages. This is the first study showing PGN-induced Ras activation may occur through the recruitment of p85α and Ras to TLR2 in RAW 264.7 macrophages. Fig. 9 is a schematic representation of the signaling pathway of PGN-induced COX-2 expression in RAW 264.7 macrophages. With an understanding of these signal transduction pathways, we can design therapeutic strategies to reduce inflammation caused by Gram-positive organisms.

REFERENCES

1. Bone, R. C. (1994) *Arch. Intern. Med.* **154,** 26–34
2. Ulevitch, R. J., and Tobias, P. S. (1995) *Annu. Rev. Immunol.* **13,** 437–457
3. Schleifer, K. H., and Kandler, O. (1972) *Bacteriol. Rev.* **36,** 407–477
4. Wang, Q., Dziarski, R., Kirschning, C. J., Muzio, M., and Gupta, D. (2001) *Infect. Immun.* **69,** 2270–2276
5. Xu, Z., Dziarski, R., Wang, Q., Swartz, K., Sakamoto, K. M., and Gupta, D. (2001) *J. Immunol.* **167,** 6975–6982
6. Bhakdi, S., Klonisch, T., Nuber, P., and Fischer, W. (1991) *Infect. Immun.* **59,** 4614–4620
7. Mattson, E., Verhage, L., Rollof, J., Fleer, A., Verhoef, J., and van Dijk, H. (1993) *FEMS Immunol. & Med. Microbiol.* **7,** 281–287
8. Wang, Z.-M., Lui, C., and Dziarski, R. (2000) *J. Biol. Chem.* **275,** 20260–20267
9. Dziarski, R., Tapping, R. I., and Tobias, P. S. (1998) *J. Biol. Chem.* **273,** 8680–8690
10. Vane, J. R., Bakhle, Y. S., and Botting, R. M. (1998) *Annu. Rev. Pharmacol. Toxicol.* **38,** 97–120
11. DeWitt, D. L. (1991) *Biochim. Biophys. Acta* **1083,** 121–134
12. Xie, W. L., Chipman, J. G., Roberstone, D. L., Erikson, R. L., and Simmons, D. L. (1991) *Proc. Natl. Acad. Sci. U. S. A.* **88,** 2692–2696
13. Mitchell, J. A., Larkin, S., and Williams, T. J. (1995) *Biochem. Pharmacol.* **50,** 1535–1542
14. Chiang, L. L., Kuo, C. T., Wang, C. H., Lee, H. M., Ho, Y. S., Kuo, H. P., and Lin, C. H. (2003) *J. Pharm. Pharmacol.* **55,** 115–123
15. Mitchell, J. A., Akarasereenont, P., Thiemermann, C., Flower, R. J., and Vane, J. R. (1993) *Proc. Natl. Acad. Sci. U. S. A.* **90,** 11693–11697
16. Lin, C. H., Kuan, I. H., Lee, H. M., Lee, W. S., Sheu, J. R., Ho, Y. S., Wang, C. H., and Kuo, H. P. (2001) *Br. J. Pharmacol.* **134,** 543–552
17. Maier, J. A., Hla, T., and Maciag, T. (1990) *J. Biol. Chem.* **265,** 10805–10808
18. Samad, T. A., Moore, K. A., Sapirstein, A., Billet, S., Allchorne, A., Poole, S., Bonventre, J. V., and Woolf, C. J. (1994) *Nature* **410,** 471–475
19. Hinz, B., and Brune, K. (2002) *J. Pharmacol. Exp. Ther.* **300,** 367–375
20. Inoue, H., Yokoyama, C., Hara, C., Tone, Y., and Tanabe, T. (1995) *J. Biol. Chem.* **270,** 24965–24971
21. Kim, Y., and Fischer, S. M. (1998) *J. Biol. Chem.* **273,** 27686–27694
22. Reddy, S. T., Wadleigh, D. J., and Herschman, H. R. (2000) *J. Biol. Chem.* **275,** 3107–3113
23. Baldwin, A. S., Jr. (1996) *Annu. Rev. Immunol.* **14,** 649–683
24. Thompson, J. L., Phillips, R. J., Bromage, H. E., Tempst, P., and Ghosh, S. (1995) *Cell* **80,** 573–582
25. DiDonato, J. A., Hayakawa, M., Rothwarf, D. M., Zandi, E., and Karin, M. (1997) *Nature* **388,** 548–554
26. Maniatis, T. (1997) *Science* **278,** 818–819
27. Woronicz, J. D., Gao, X., Cao, Z., Rothe, M., and Geoddel, D. (1997) *Science* **278,** 866–869
28. Chen, Z., Hagler, J., Palombella, V. J., Melandri, F., Scherer, D., Ballard, D., and Maniatis, T. (1995) *Genes Dev.* **9,** 1586–1597
29. Campbell, S. L., Khosravi-Far, R., Rossman, K. L., Clark, G. J., and Der, C. J. (1998) *Oncogene* **17,** 1395–1413
30. Blaine, S., Wick, M., Dessev, C., and Nemenoff, R. A. (2001) *J. Biol. Chem.* **276,** 42737–42743
31. Subbaramaiah, K., Norton, L., Gerald, W., and Dannenberg, A. J. (2002) *J. Biol. Chem.* **277,** 18649–18657
32. Marshall, C. J. (1996) *Curr. Opin. Cell Biol.* **8,** 197–204
33. Zang, M., Hayne, C., and Luo, Z. (2002) *J. Biol. Chem.* **277,** 4395–4405
34. Zhang, X.-F., Settleman, J. M., Takeuchi-Suzuki, E., Ellsdge, S. J., Marshall, M. S., Bruder, J. T., Rapp, U. R., and Avruch, J. (1993) *Nature* **364,** 308–313
35. Whitmarsh, A. J., and Davis, R. J. (1998) *Trends Biochem. Sci.* **23,** 481–485
36. Lin, C. H., Sheu, S. Y., Lee, H. M., Ho, Y. S., Lee, W. S., Ko, W. C., and Sheu, J. R. (2000) *Mol. Pharmacol.* **57,** 36–43
37. Chen, B.-C., Chou, C.-H., and Lin, W.-W. (1998) *J. Biol. Chem.* **273,** 29754–29763
38. Pierce, J. W., Schoenleber, R., Jesmok, G., Best, J., Moore, S. A., Collins, T., and Gerritsen, M. E. (1997) *J. Biol. Chem.* **272,** 21096–21103
39. Wu, M., Lee, H., Bellas, R. E., Schauer, S. L., Arsura, M., Katz, D., FitzGerald, M. J., Rothstein, T. L., Sherr, D. H., and Sonenshein, G. E. (1996) *EMBO J.* **15,** 4682–4690
40. Musial, A., and Eissa, N. T. (2001) *J. Biol. Chem.* **276,** 24268–24273
41. Hara, M., and Han, M. (1995) *Proc. Natl. Acad. Sci. U. S. A.* **92,** 3333–3337
42. Varga, E. V., Rubenzik, M., Grife, V., Sugiyama, M., Stropova, D., Roeske, W. R., and Yamamura, H. I. (2002) *Eur. J. Pharmacol.* **451,** 101–102
43. Frost, J. A., Steen, H., Shapiro, P., Lewis, T., Ahn, N., Shaw, P. E., and Cobb, M. H. (1997) *EMBO J.* **16,** 6426–6438
44. Lee, H.-W., Ahn, D.-H., Crawley, S. C., Li, J.-D., Gun, J. R., Jr., Basbaum, C. B., Fan, N. Q., Szymkowaski, D. E., Han, S.-Y., Lee, B. H., Sleisenger, M. H., and Kim, Y. S. (2002) *J. Biol. Chem.* **277,** 32624–32631
45. Arbibe, L., Mira, J. P., Teusch, N., Kline, L., Guha, M., Mackman, N., Godowiski, P. J., Ulevitch, R. J., and Knaus, U. G. (2000) *Nat. Immun.* **1,** 533–540
46. Baeuerle, P. A., and Henkel, T. (1994) *Annu. Rev. Immunol.* **12,** 141–179
47. Hwang, D., Jang, B. C., Yu, G., and Boudreau, M. (1997) *Biochem. Pharmacol.* **54,** 87–96
48. Rhee, S. H., and Hwang, D. (2000) *J. Biol. Chem.* **275,** 34035–34040
49. Heiss, E., Herhaus, C., Klimo, K., Bartsch, H., and Gerhauser, C. (2001) *J. Biol. Chem.* **276,** 32008–32015
50. Yadav, P. N., Liu, Z., and Rafi, M. M. (2003) *J. Pharmacol. Exp. Ther.* **305,** 925–931
51. Elgavish, A. (2000) *J. Cell. Physiol.* **182,** 232–238
52. Arsura, M., Mercurio, F., Oliver, A. L., Thorgeirsson, S. S., and Sonenshein, G. E. (2000) *Mol. Cell. Biol.* **20,** 5381–5391
53. O'Nell, L. (2000) *Biochem. Soc. Trans.* **28,** 557–563
54. Vasselon, T., and Detmers, P. A. (2002) *Infect. Immun.* **70,** 1033–1041
55. Horng, T., Barton, G. M., Flavell, R. A., and Medzhitov, R. (2002) *Nature* **420,** 329–333
56. Yeo, S.-J., Yoon, J.-G., and Yi, A.-K. (2003) *J. Biol. Chem.* **278,** 40590–40600
57. Palsson, E. M., Popoff, M., Thelestam, M., and O'Nell, A. J. (2000) *J. Biol. Chem.* **275,** 7818–7825
58. McDermott, E. P., and O'Neill, L. A. (2002) *J. Biol. Chem.* **277,** 7808–7815
59. Sheng, H., Shao, J., and DuBois, R. N. (2001) *Cancer Res.* **61,** 2670–2675
60. Xie, W., Fletcher, B. S., Andersen, R. D., and Herschman, H. R. (1994) *Mol. Cell. Biol.* **14,** 6531–6539
61. Geppert, T. D., Whitehurst, C. D., Thompson, P., and Beutler, B. (1994) *Mol. Med.* **1,** 93–103
62. Lin, C. H., Kuan, I. H., Wang, C. H., Lee, W. S., Sheu, J. R., Hsiao, G., Wu, C. H., and Kuo, H. P. (2002) *Eur. J. Pharmacol.* **450,** 1–9
63. Frost, J, A., Swantek, J. L., Stippec, S., Yin, M. J., Gaynor, R., and Cobb, M. H. (2000) *J. Biol. Chem.* **275,** 19693–19699
64. Pahan, K., Sheikh, F. G., Namboodiri, A. M., and Singh, I. (1997) *J. Clin. Investig.* **100,** 2671–2679
65. Paul, A., Cuenda, A., Bryant, C. E., Murray, J., Chilveers, E. R., Cohen, P., Gould, G. W., and Plevin, R. (1999) *Cell. Signal.* **11,** 491–497
66. Wadleigh, D. J., Reddy, S. T., Kopp, E., Ghosh, S., and Herschman, H. R. (2000) *J. Biol. Chem.* **275,** 6259–6266